NATIONAL AERONAUTICS AND SPACE ADMINISTRATION

EARTH RESOURCES SURVEY PROGRAM

TECHNICAL LETTER NASA-95

A SURVEY OF LUNAR GEOLOGY

By

Jerald J. Cook
Willow Run Laboratories
Institute of Science and Technology
Ann Arbor, Michigan

November 1967

Prepared by the Geological Survey for the
National Aeronautics and Space Administration (NASA)
under NASA Contract No. R-146-09-020-006

MANNED SPACECRAFT CENTER
HOUSTON, TEXAS

UNITED STATES
DEPARTMENT OF THE INTERIOR
GEOLOGICAL SURVEY
WASHINGTON, D.C. 20242

Interagency Report
NASA-95
November 1967

Colonel Michael Ahmajan
Acting Chief, Earth Resources
  Discipline Surveys
Office of Space Science and Applications
Code SAR - NASA Headquarters
Washington, D.C. 20546

Dear Colonel Ahmajan:

Transmitted herewith is one copy of:

INTERAGENCY REPORT NASA-95

A SURVEY OF LUNAR GEOLOGY*

by

Jerald J. Cook**

The U.S. Geological Survey has released this report in open files. Copies are available for consultation in the Geological Survey Libraries, 1033 GSA Building, Washington, D.C. 20242; Building 25, Federal Center, Denver, Colorado 80225; and 345 Middlefield Road, Menlo Park, California 94025.

Sincerely yours,

William A. Fischer
Research Coordinator
Earth Orbiter Program

*Work performed under NASA Contract No. R-146-09-020-006
**Willow Run Laboratories of the Institute of Science and Technology, University of Michigan, Ann Arbor, Michigan

UNITED STATES

DEPARTMENT OF THE INTERIOR

GEOLOGICAL SURVEY

INTERAGENCY REPORT NASA-95

SURVEY OF LUNAR GEOLOGY*

by

Jerald J. Cook**

November 1967

The work reported herein was conducted by the Willow Run Laboratories of the Institute of Science and Technology, University of Michigan on behalf of the U.S. Geological Survey, Branch of Theoretical Geophysics, under Contract 14-09-001-10108

*Work performed under NASA Contract No. R-146-09-020-006

**Willow Run Laboratories of the Institute of Science and Technology, University of Michigan, Ann Arbor, Michigan

FOREWORD

The work described in this report was conducted by the Infrared and Optical Sensor Laboratory (M. R. Holter, Head) of Willow Run Laboratories, a unit of The University of Michigan's Institute of Science and Technology. D. S. Lowe was the Principal Investigator. The work reported here is consonant with and fulfills part of the objectives of a comparative multispectral remote-sensing program of the Infrared and Optical Sensor Laboratory. The goal of the program is to develop methods of improving and extending current remote-sensing capabilities by studying the spectral characteristics of surface features of objects being sought. Improvements are being sought in the kinds and quantities of data obtainable and in the quality, speed, and economy of the image-interpretation process. The present study is very closely related to and dependent upon other studies completed by Willow Run Laboratories under contract to the U. S. Geological Survey (Contract No. 14-80-0001-10053) and under contract to the National Aeronautics and Space Administration (Contract No. NAS8-21000). Previous related reports issued by the Infrared and Optical Sensor Laboratory are listed on the following pages.

RELATED REPORTS

COMPARATIVE MULTISPECTRAL SENSING (U), M. R. Holter and F. C. Polcyn, Report No. 2900-484-R, Willow Run Laboratories of the Institute of Science and Technology, The University of Michigan, Ann Arbor, June 1965, AD 362 283 (CONFIDENTIAL).

DIURNAL AND SEASONAL VARIATIONS IN RADIATION OF OBJECTS AND BACKGROUNDS, 4.5-5.5-μ SPECTRAL REGION (U), L. D. Miller and R. Horvath, Report No. 6400-32-T, Willow Run Laboratories of the Institute of Science and Technology, The University of Michigan, Ann Arbor, June 1965, AD 362 620 (CONFIDENTIAL).

THE INVESTIGATION OF A METHOD FOR REMOTE DETECTION AND ANALYSIS OF LIFE ON A PLANET, M. R. Holter, D. S. Lowe, and R. J. Shay, Report No. 6590-1-P, Institute of Science and Technology, The University of Michigan, Ann Arbor, November 1964.

SPECTRUM MATCHING (U), R. E. Hamilton, Report No. 6400-18-T, Willow Run Laboratories of the Institute of Science and Technology, The University of Michigan, Ann Arbor, June 1965, AD 363 001 (CONFIDENTIAL).

TARGET SIGNATURE STUDY, INTERIM REPORT, VOLUME I: SURVEY (U), R. R. Legault and T. Limperis, Report No. 5698-22-T(I), Institute of Science and Technology, The University of Michigan, Ann Arbor, October 1964, AD 354 166 (CONFIDENTIAL).

TARGET SIGNATURE STUDY, INTERIM REPORT, VOLUME II: RECOMMENDATIONS (U), R. R. Legault and T. Limperis, Report No. 5698-22-T(II), Institute of Science and Technology, The University of Michigan, Ann Arbor, October 1964 (CONFIDENTIAL).

TARGET SIGNATURE STUDY, INTERIM REPORT, VOLUME III: POLARIZATION (U), R. R. Legault and T. Limperis, Report No. 5698-22-T(III), Institute of Science and Technology, The University of Michigan, Ann Arbor, October 1964, AD 354 025 (CONFIDENTIAL).

TARGET SIGNATURE STUDY, INTERIM REPORT, VOLUME IV: BIBLIOGRAPHY (ACOUSTIC, ULTRAVIOLET, VISIBLE, INFRARED, AND RADAR) (U), T. Limperis and R. S. Gould, Report No. 5698-22-T(IV), Institute of Science and Technology, The University of Michigan, Ann Arbor, October 1964, AD 354 232 (SECRET).

TARGET SIGNATURE STUDY, INTERIM REPORT, VOLUME V: CATALOG OF SPECTRAL REFERENCE DATA, R. R. Legault, R. S. Gould, and T. Limperis, Report No. 5698-22-T(V), Institute of Science and Technology, The University of Michigan, Ann Arbor, October 1964.

A COMPREHENSIVE TARGET-SIGNATURE MEASUREMENT PROGRAM, FIRST INTERIM TECHNICAL REPORT, VOLUME I: TECHNICAL DISCUSSION (U), Report No. 7251-3-P(I), Willow Run Laboratories of the Institute of Science and Technology, The University of Michigan, Ann Arbor, December 1965 (CONFIDENTIAL).

A COMPREHENSIVE TARGET-SIGNATURE MEASUREMENT PROGRAM, SECOND INTERIM TECHNICAL REPORT, VOLUME I: DATA PROCESSING, STORAGE, AND ANALYSIS (U), Report No. 7251-9-P(I), Willow Run Laboratories of the Institute of Science and Technology, The University of Michigan, Ann Arbor, June 1966 (CONFIDENTIAL).

A COMPREHENSIVE TARGET-SIGNATURE MEASUREMENT PROGRAM, SECOND INTERIM TECHNICAL REPORT, VOLUME II: MEASUREMENT IMPLEMENTATION (U), Report No. 7251-9-P(II), Willow Run Laboratories of the Institute of Science and Technology, The University of Michigan, Ann Arbor, June 1966 (CONFIDENTIAL).

A COMPREHENSIVE TARGET-SIGNATURE MEASUREMENT PROGRAM, THIRD INTERIM TECHNICAL REPORT (U), Report No. 7251-15-P, Willow Run Laboratories of the Institute of Science and Technology, The University of Michigan, Ann Arbor, February 1966 (CONFIDENTIAL).

A COMPREHENSIVE TARGET-SIGNATURE MEASUREMENT PROGRAM, FINAL REPORT (U), T. Limperis, Report No. 7251-21-F, Willow Run Laboratories of the Institute of Science and Technology, The University of Michigan, Ann Arbor, December 1966, AD 378 112 (CONFIDENTIAL).

DISPERSIVE MULTISPECTRAL SCANNING: A FEASIBILITY STUDY, FINAL REPORT, J. Braithwaite, Report No. 7610-5-F, Willow Run Laboratories of the Institute of Science and Technology, The University of Michigan, Ann Arbor, September 1966.

AN INVESTIGATIVE STUDY OF A SPECTRUM-MATCHING IMAGING SYSTEM, FINAL REPORT, D. S. Lowe, J. Braithwaite, and V. L. Larrowe, Report No. 8201-1-F, Willow Run Laboratories of the Institute of Science and Technology, The University of Michigan, Ann Arbor, October 1966.

TARGET SIGNATURES ANALYSIS CENTER: DATA COMPILATION, D. G. Earing and J. A. Smith, Report No. 7850-2-B, Willow Run Laboratories of the Institute of Science and Technology, The University of Michigan, Ann Arbor, July 1966, AD 489 968.

INVESTIGATION OF SPECTRUM-MATCHING SENSING IN AGRICULTURE, SEMIANNUAL REPORT (U), F. C. Polcyn, Report No. 6590-7-P, Willow Run Laboratories of the Institute of Science and Technology, The University of Michigan, Ann Arbor, in publication; Vol. I, UNCLASSIFIED; Vol. II, CONFIDENTIAL.

OPTICAL SENSING OF THE MOISTURE CONTENT IN FINE FOREST FUELS, FINAL REPORT, C. E. Olson, Jr., Report No. 8036-1-F, Willow Run Laboratories of the Institute of Science and Technology, The University of Michigan, Ann Arbor, in publication.

ABSTRACT

The literature of lunar science has been surveyed. Those aspects of the survey relevant to experiments involving optical-mechanical radiometers and scanners used in lunar orbit are reported. An account of the current theories of the nature of the lunar surface is given. Accounts are also given of previous work related to the photometric function, color, and apparent temperature, and the various anomalies in these areas. The work supporting the possibility of identifying surface rocks on the basis of their infrared reflectance spectra is described in an appendix.

No conclusions can be drawn other than that the interpretation of the existing experimental data leads to many ambiguities. Thus any experiments which might provide more information would be welcome.

CONTENTS

FIGURES

TABLES

A SURVEY OF LUNAR GEOLOGY
10 January 1966 Through 10 June 1966

1
INTRODUCTION

The original work statement on this contract required the contractor to ". . . make an engineering feasibility study of a lunar orbiting scanning radiometer leading to the definition of feasible infrared experiments. . . ." Later the work statement was altered to require emphasis on technological problems and earth-orbiting experiments.

Early in the study under the original work statement, it became apparent that while a number of experiments and equipments had been proposed, the uncertainty and disagreement on the nature and history of the lunar surface is such that it was far from clear which experiment or experimental parameters would be of greatest value. It was therefore decided to carry out a survey of the scientific literature relating to the moon in order to uncover the ways in which radiometry from orbit might elucidate matters and further to determine what equipment specifications would be of greatest and most general value.

The state of lunar science at the close of the study has become even more uncertain than it was at the start. For example, whereas most deductions from earth-based observations indicated, or at least were consistent with, the theory that the surface of the moon is a dust layer of unknown thickness, the results of the early photographs telemetered back from the lunar landers indicate a somewhat cohesive soil-like surface. It is clear that much remains to be done. While contact exploration and high-resolution photography will undoubtedly play a leading role, any other techniques which can shed light on this intriguing and presently paradoxical subject will also play a role; among these optical-mechanical radiometry will surely have an important place.

2
A "PROBABLE" LUNAR SURFACE MODEL

After more than three and one-half centuries of observation and compilation of pertinent data, it is still impossible to state definitive and final conclusions as to the character of lunar surface detail. Much of the confusing and conflicting interpretation arises from the fact that all evidence for the physical nature of the surface has been obtained indirectly, through inferences drawn from the characteristics of reflected and emitted radiation. With the exception of the highly localized glimpses provided by Rangers VII, VIII, and IX and Surveyor I, all conclusions regarding the lunar surface are drawn from earth-based telescopic observations wherein the best resolution corresponds to about 750 m photographically and 200 m visually [1]. In general, the average characteristics of large areas of lunar terrain have then been compared with the behavior of laboratory-sized samples of various terrestrial materials.

Despite the obvious difficulties and many dissenting opinions, it is possible to reach what might be termed a "most probable" lunar surface model. It should be noted, however, that perhaps no single facet of such an average model enjoys universal acceptance. Essentially, every aspect of surface detail has been explained by a variety of often conflicting theories. Nevertheless, most authors tend to accept (with their own minor modifications) a great many of the more conservative inferences leading to a probable surface model. Recent data indicate that certain of these inferences may be superfluous in the explanation of observed phenomena. However, the inertia of centuries of observation and debate acts effectively to dampen any rapid change in the evolving model.

The essential characteristics observed in the emitted and reflected radiation which bear upon our interpretation of the physical nature of the lunar surface may be summarized as follows.

(1) The lunar albedo varies from place to place sufficiently to produce the readily discernible distinction between the highlands and the maria, but it is quite uniform relative to differences in reflectivity of terrestrial rocks. The small and nearly uniform albedo suggests the effect of an infall of a dark or subsequently darkened cosmic dust, possibly mixed with local debris from crater formation. The depth of such a layer and reasons for even a slight albedo variation are largely hypothetical, depending upon estimated infall rates and various transport theories.

(2) The overall color differences are negligibly small, the lunar surface being everywhere a dark grayish brown. Lunar surface materials occupy a small region of the color-brightness diagram essentially devoid of any known terrestrial materials. This again suggests a rather uniform infall of cosmic material, perhaps regionally affected by a mixture of local material.

(3) The polarization of light reflected from the lunar surface has been found to agree with few exceptions to that of a dark, absorbing powder similar to a fine volcanic ash or an opaque dust. Although there is some variation in the degree of polarization (inversely with albedo) over the lunar surface, the otherwise marked similarity indicates a common dust covering.

(4) The visible reflectance function (i.e., the variation in brightness with phase) of the entire lunar disk, as well as every element of the surface, is extremely steep near full moon; there is no limb darkening. In an attempt to account for this peculiar photometric behavior, hypothetical complex and highly vesicular structures, replete with innumerable pits and inter-

connected cavities, have been devised. Laboratory studies indicate that some of the more complex models do, in fact, closely approximate the lunar reflectance curve. However, recent data indicate that such elaborate and improbable models may be unnecessary, as a great many (perhaps nearly all) terrestrial materials exhibit similar properties when viewed under appropriate conditions closely approximating those of the full-moon situation. Nevertheless, the more generally accepted probable model must be said to include a highly visculated surface of complex microstructure, creating innumerable interconnected cavities and consisting predominantly of voids. Rationalizing this fact with the well-supported blanket of dust has been accomplished only through the "fairy-castle" structures of Hapke [2].

(5) Infrared and microwave measurements of apparent surface and subsurface temperature variations during an eclipse as well as a normal lunation indicate a thermal conductivity far below that of any known solid substance. Analysts of these data have concluded that the surface is covered by a layer of loosely compacted dust or rock powder in which conduction can be effected only through minute point contacts.

(6) Radar echoes indicate that the surface is essentially smooth to gently undulating, with gradients no larger than 1 in 10 to 1 in 20 in an area of a few centimeters to a meter. Current measurements at 3.6 cm indicate that only about 14% of the surface is covered by objects of a size on the order of the wavelength.

Thus a probable lunar surface model is essentially smooth (certainly smooth compared to the curvature of the lunar globe) and monotonously drab and desolate. The microrelief may possibly (although not necessarily) exhibit considerable structure on the scale of a millimeter or less. The one apparently essential feature, indicated by nearly every characteristic examined, is the presence of an all-covering layer of dust, possibly in varying thickness and at various angles of repose. This material is presumed to originate from cosmic infall mixed with local debris, varying from large-block rubble to rock flour.

The overwhelming evidence of a lunar dust layer is unique in the widespread support offered by measurements from different disciplines. In no other case do the data so consistently indicate a particular characteristic. It is ironic that all high-resolution observations available to date (Luna 9, Rangers VII, VIII, and IX, and Surveyor I) can be interpreted to indicate the absence of a dust layer. In fact, Kuiper [3, 4] concluded from his interpretation of Ranger data that the maria consist mainly of large-scale lava flows which are not covered by dust. However, Gold interpreted the same data (specifically Ranger VII photographs) to "have clearly strengthened the case for dust as the main constituent of the lunar lowlands by not showing any rock formations" [5, p. 7]. Jaffe views the same photographs as indicating an overlay of "dust or other granular material . . . at least 5 meters thick . . . and perhaps considerably thicker" [6, pp. 6129-6138]. Surveyor I indicated the surface of its site in Oceanus Procellarum to be covered by a finely granulated, somewhat cohesive soil-like material, but not dust [7].

3
THE ALBEDO AND COLOR OF THE LUNAR SURFACE

The relative brightness of lunar surface features is given in terms of their normal albedo, or the ratio of their brightness to that of a perfectly reflecting Lambertian surface, both surfaces being illuminated and viewed normally. The lunar albedo is uniformly low, averaging about 0.09, while varying from place to place from a minimum of 0.05 for the darkest maria and certain dark craters to a maximum of about 0.18 for the brightest parts of the crater Aristarchus (see table I for values of albedo of various representative features). Thus the ratio of the intensity of the brightest and darkest lunar details is just over 3, while, on the average, the bright mountainous areas are no more than 1.8 times as bright as the darker maria. This variation, while readily discernible, is quite small compared to the differences in reflectivity of terrestrial rocks which can vary by a factor of 50 or more.

The nearly uniform lunar albedo has been used by Kopal [9] to argue the presence of a blanket of cosmic dust, mixed with local debris from crater formation. However, other authors feel that such a dust cover would necessarily wipe out all traces of difference and contend that the effect of dust originating outside the moon is minor [10].

TABLE 1. ALBEDO OF VARIOUS LUNAR FEATURES [8]

Representative Object	Albedo
Floor of Grimaldi and Riccioli	0.061
Floor of crater Boscovich	0.067
Floor of Julius Caesar and Endymion	0.074
Floor of Pitatus and Marius	0.081
Floor of Taruntius, Plinius, Flamsteed, Theophilus, and Mercator	0.088
Floor of Hansen, Archimedes, and Mersenius	0.095
Floor of Ptolemaeus, Manilius, and Guericke	0.102
Environs of Aristillus	0.109
Wall of Arago, Landsberg, Bullialdus, and the neighborhood of Kepler	0.115
Wall of Picard, Timocharis, the rays of Copernicus	0.122
Wall of Macrobius, Kant, Bessel, Mösting, and Flamsteed	0.129
Wall of Lagrange, La Hire, and Theatetus	0.135
Wall of Feon Jun., Ariadaeus, Behaim, and Bode B	0.142
Wall of Euclides, Ukert, and Hortensius	0.149
Wall of Godin, Copernicus, and Bode	0.156
Wall of Proclus, Bode A, and Hipparchus C	0.163
Wall of Mersenius, and Mösting A	0.169
Interior of Aristarchus	0.176
Central mountain of Aristarchus	0.183

A comparison of lunar albedo values with those of known terrestrial materials shows the latter to be, in general, much higher. The notable exceptions, volcanic slag (with a mean albedo of 0.06) and the fusion crust of meteorites (0.05), were called upon by Sytinskaya to support the meteor-slag theory, in which the slaggy surface of the maria is predominantly ultrabasic while the continents are basic-basic. Albedo differences are felt to result from meteoric bombardment. Sytinskaya [11] explains the dark color of other bodies such as Mercury in an analogous manner.

In terrestrial materials, the albedo has a pronounced effect upon polarization; the maximum of the positive polarization (P_{max}) is inversely related to albedo. The moon is unique, compared to most terrestrial materials, combining a low P_{max} with a low albedo (see fig. 1).

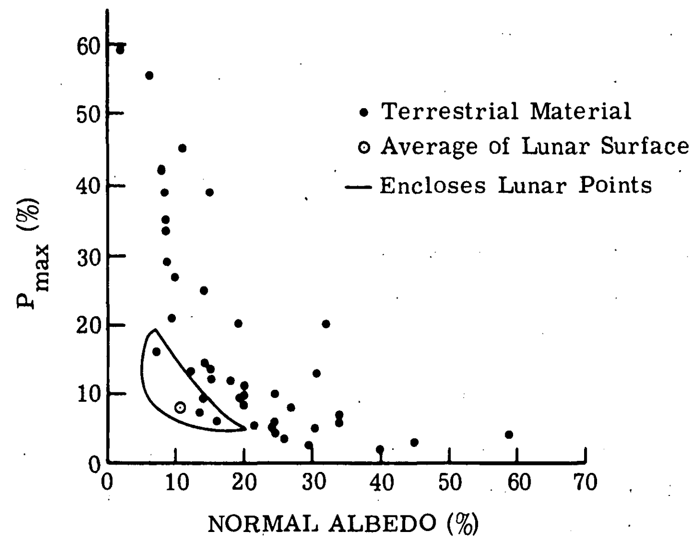

FIGURE 1. POLARIZATION-BRIGHTNESS DIAGRAM FOR LUNAR AND TERRESTRIAL MATERIALS [2]

There are innumerable areas of different brightness on the lunar surface, and in some cases their relative orientation (such as overlapping) has been used to establish relative ages for the various features. For example, the bright rays associated with certain craters extend outward from the crater rim, overriding neighboring features, suggestive of a huge splash of material from the crater site. All gradations may be observed in the brightness of the rays associated with different craters. Copernicus, Aristilles, and Theophilus illustrated this effect with the rays of Copernicus extending more than 300 mi outward from the rim in bright arcs and loops across the dark maria, the rays of Aristilles are plainly visible but less bright, and those of Theophilus are extremely dim. Rayless craters, or those with faint rays, occurring in a system of brighter rays are invariably superimposed on it. In all cases, the brighter rays appear to be associated with more recent events, indicating that a darkening process is causing a fading of the brighter lunar features [12].

The treatment which exposed lunar material has received is very different from that of terrestrial rocks, providing several reasons for this apparent darkening with age. Hapke and Van Horn [13] note that repeated shocking by impact and prolonged exposure to high-energy cosmic radiation will result in a highly disordered lattice of higher opacity. Wehner [14] reports that repeated ion bombardment (as by the hydrogen ions of the solar wind) darkens insulators with rough surfaces. The infall of a cosmic material of very low albedo (similar to the dark zodiacal cloud suggested by Kopal [9]) could produce the observed effect.

Whatever the underlying causes, there is considerable circumstantial evidence that exposure to the lunar environment results in a gradual darkening of the surface material and that subsurface material is initially brighter. Contrary to this conclusion, the average albedo of ejected material, photographed near the footpads of Surveyor I, was nearly 30% lower than that of the undisturbed surface [7]. The landing site, in a dark part of Oceanus Procellarum, is described as "bland" with an albedo (estimated from earth-based observation) of about 0.052 [7]. The area does not appear to be overlain by any of the various bright ray systems. The reasons for the underlying (hence protected) material to appear significantly darker than the undisturbed surface are not clear.

The very small difference in color exhibited by various regions of the lunar surface also indicates the uniformity of its outer covering. Sharanov [15] has studied lunar color differences based upon a color excess D defined as the difference between the color index of a given object and that of the sun. Table II gives values of albedo and color excess determined for various lunar features and terrestrial materials. Color-excess values for lunar features largely fall around 0.35 with extremes no greater than ±0.06, a rather uniform and dull brownish gray.* The color dispersion across the maria and dark features is somewhat larger than in the brighter highlands, but Sharanov states that "a careful and repeated study under great magnification . . . did not reveal a single, even small, object whose color appreciably differed from that of the background" [15, p. 388]. Data similar to those in table II have been used to construct color-brightness diagrams for lunar and terrestrial materials [17] such as the one shown in figure 2.

Any attempt to identify lunar materials by their observed position on the color-brightness diagram assumes that materials of similar mineralogical and petrographic composition in the

*With this color-excess system, proposed by King [16], D = 0 describes a gray substance, bluish colors yield negative values, and yellow, brown, and reddish materials will be positive [15, p. 388].

TABLE II. ALBEDO AND COLOR EXCESS OF VARIOUS LUNAR FEATURES AND TERRESTRIAL MATERIALS [15]

Type of Object or Material	Albedo			Color Excess (D)		
	Average	Extreme		Average	Extreme	
Moon, maria, and floors of dark cirques	0.065	0.05	0.08	+0.339	+0.29	+0.40
Moon, pali	0.091	0.09	0.10	+0.349	+0.31	+0.37
Moon, continents, and floors of craters with normal coloring	0.105	0.08	0.12	+0.347	+0.31	+0.38
Bright rays and craters with bright floors	0.140	0.10	0.18	+0.352	+0.31	+0.39
All parts of moon together	0.090	0.05	0.18	+0.344	+0.29	+0.40
Volcanic slag, scorias	0.060	0.02	0.14	+0.11	-0.13	+1.28
Volcanic tuff	0.193	0.06	0.43	+0.29	-0.15	+1.10
Pumice	0.354	0.13	0.55	+0.43	+0.05	+0.81
Dunite, peridotite	0.104	0.06	0.16	-0.01	-0.17	+0.25
Gabbro, norite	0.155	0.08	0.21	-0.04	-0.17	+0.12
Basalt	0.133	0.06	0.28	-0.05	-0.31	+0.15
Diabase	0.151	0.11	0.19	-0.02	-0.19	+0.13
Andesite	0.139	0.08	0.31	-0.02	-0.12	+0.10
Granite	0.244	0.04	0.70	+0.39	-0.09	+1.23
Metamorphic rocks	0.281	0.08	0.78	+0.26	-0.25	+0.99
Clays and schists	0.251	0.12	0.50	+0.33	-0.24	+1.53
Sand	0.240	0.10	0.40	+0.49	+0.06	+1.22
Sandstone	0.222	0.06	0.54	+0.66	+0.03	+1.54
Limonite, ortstein	0.131	0.05	0.35	+0.69	0.00	+1.24
Limestone, marl	0.325	0.06	0.80	+0.38	-0.13	+1.52
Stone meteorites	0.183	0.04	0.48	+0.10	-0.16	+0.36
Fusion crust of meteorites	0.052	0.02	0.17	+0.11	-0.10	+0.38

lunar and terrestrial environments will exhibit similar properties. The validity of such an assumption is doubtful, considering the vast differences in the two environments. A small amount of "foreign" contaminating material, or minor changes caused by radiation or ion bombardment, may well mask otherwise recognizable features.

The large field of view over which telescopic measurements are averaged also tends to mask or obscure local color-brightness variations. These large areal observations are then compared with similar properties deduced from the measurement of laboratory-sized terrestrial samples. As is frequently the case in earth-based lunar investigation, we can only observe that, on the average, lunar materials occupy a portion of the color-brightness diagram which is essentially devoid of terrestrial materials.

Recent reports by Sharanov [18] and Sytinskaya [19] indicate that various porous and loose substances emitted by active terrestrial volcanoes generally correspond to the lunar albedo

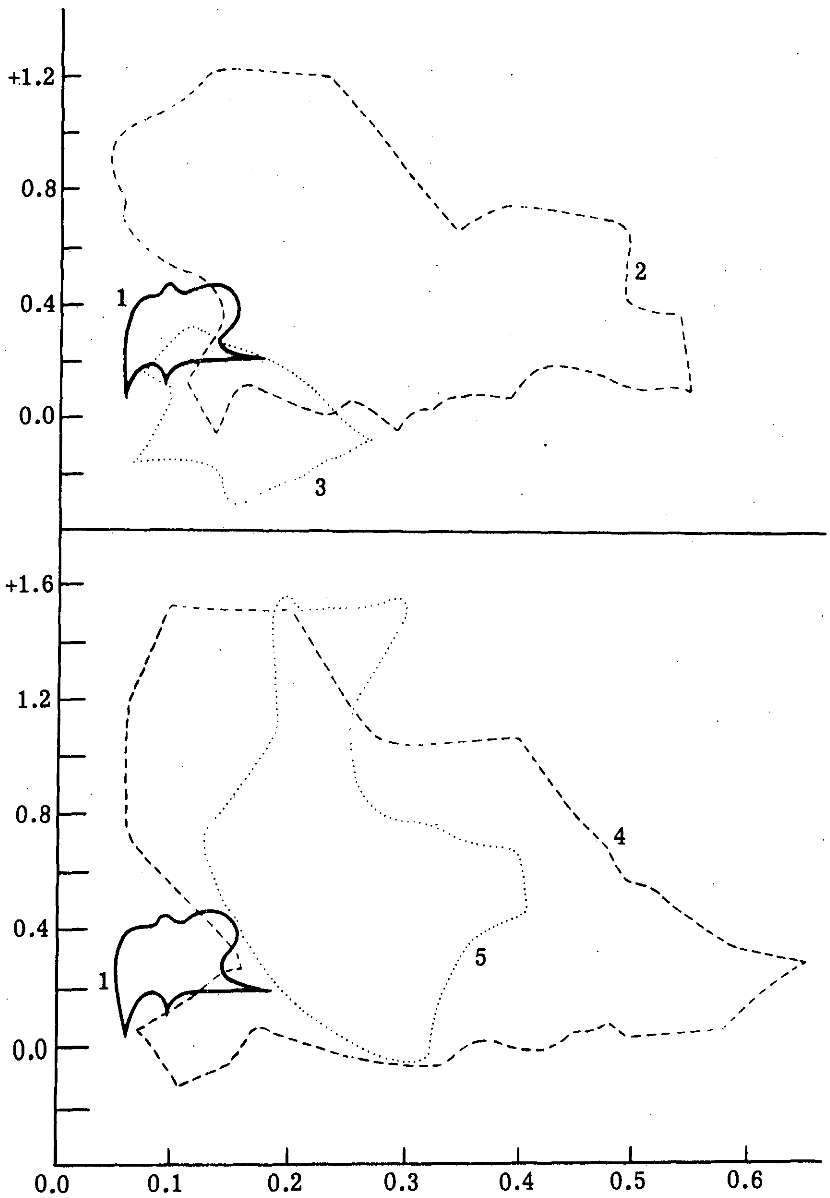

FIGURE 2. COLOR-BRIGHTNESS DIAGRAMS FOR LUNAR DETAILS AND FOR VARIOUS TERRESTRIAL SPECIMENS. Line 1: lunar; 2, 3, 4, and 5: terrestrial. [17]

and color. They note that a similarity in color is obtained for pyroclastic materials of the slag and lapilli type, but not for lava. Slag is said to be somewhat redder, pumice the same color, and lapilli, sand, and ash more brown, gray, or black, than the moon. They propose that by proper combination volcanic products can be shown to duplicate lunar observations.

Whether the lunar albedo and color effects arise from nonterrestrial material, from observational limitations, or from environmental effects is unknown.

4
THE LUNAR PHOTOMETRIC FUNCTION

The characteristic manner in which the lunar surface reflects insolation has presented a Gordian knot for more than three centuries. In 1632, Galileo [20] noted that at full moon lunar brightness is approximately uniform over the entire disk, i.e., there is no limb darkening. If the surface behaved as a diffuse reflector, the full moon would, of necessity, appear brighter near the center and progressively dimmer near the limb. In the early 18th century, Bouguer [21] attempted to explain this lunar reflectance phenomenon through shadows cast by very steep mountains. Thus observers have long sought, rather unsuccessfully, to establish a meaningful relation between photometric observations and lunar surface structure.

Measurements of the integral brightness of the lunar disk as a function of phase angle have been performed by many observers [e.g., 22-25]. In 1916, Russell [26] surveyed the data of previous observers, deduced mean values, and determined a phase-angle variation of integral brightness. Rougier [27], in 1933, obtained a similar phase brightness function through precise, independent measurements. Curves plotted by both Russell and Rougier are presented in figure 3. The undefined peak near zero for phase angles less than 1.5^{o} is caused by eclipsing of the moon by the earth. Because of the very steep rise near occulation, extrapolation is extremely difficult. However, what is classically termed a full moon presents twice the illuminated area of quadrature but eleven times the integral brightness. As noted recently by Gehrels et al. [28], the reflectivity may as much as double as the phase angle changes from 5^{o} to 0^{o}.

Many workers have considered the differing brightness of various lunar surface details. Barabashev in 1922 [29] first expressed the photometric homogeneity of the entire disk: not only does the moon reflect in such a way that the integral brightness reaches a sharp maximum at or near full moon, but also the apparent brightness of every detail shows a similar peak regardless of location on the disk or the type of terrain. This expression of lunar photometric behavior has been confirmed and refined through the extensive measurements by Markov [30], Opik [31], Bennett [32], and van Diggelen [33].

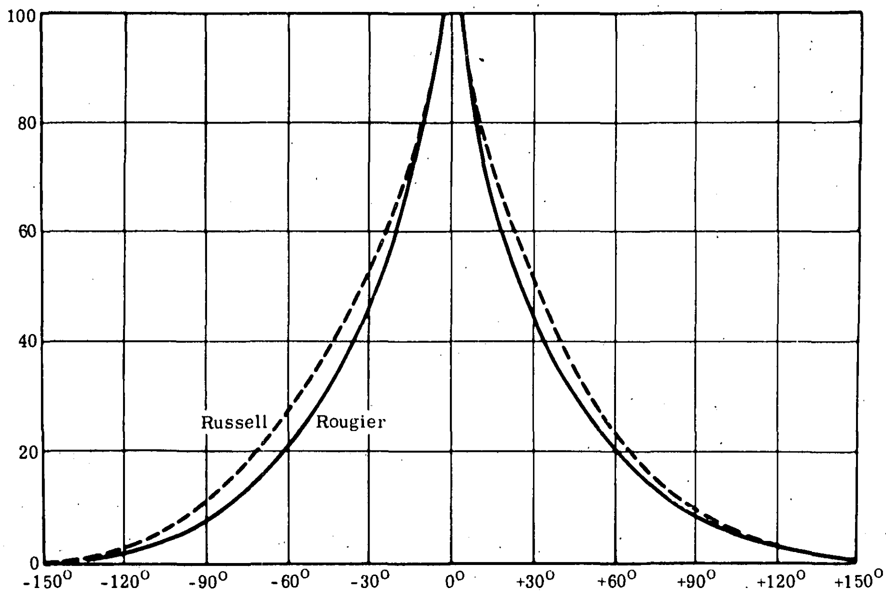

FIGURE 3. TOTAL BRIGHTNESS OF THE MOON VS. PHASE [8]

Fedoretz [34] has provided the most extensive catalog of lunar photometric data available to date. His measurements indicate that in some cases the maximum brightness is displaced away from zero phase angle toward that corresponding to solar zenith for the given surface detail (e.g., the craters Tycho and Copernicus). Fedoretz also determined that the bright rays and certain bright craters differ from the more general reflectance function by exhibiting an even more pronounced peak near zero phase. This observation has been recently confirmed by the photoelectric measurements of Wildey and Pohn [35].

Many theoretical attempts have been made to predict the moon's photometric behavior. Most models have suggested a surface covered by cracks [29], rocks or domes [36], cups or craters [32, 33], volcanic foam [37], or steep-walled cavities [38]. Theories have in general tended toward a terrestrially familiar structure of well-known materials such as sands, rocks, and volcanic products. The failure of most models to satisfactorily duplicate the lunar reflection law may result in part from the peculiar environmental conditions imposed on lunar surface materials. However, recent evidence (discussed more fully below) indicates that it is more likely the result of instrumental limitations in evaluating the experimental models. Extensive laboratory investigations on a large variety of terrestrial materials and structural forms have been reported [13, 33, 39-43].

While Orlova [39] was able to obtain a reflectance maximum in the direction of the incident beam for certain volcanic tuffs, she found the moon to exhibit a very much greater elongation toward the source. Van Diggelen found that the agglomerated volcanic ash, strongly suggested by polarization studies, did not conform to his lunar observations. He concluded that the surface compares most favorably with a highly complex structure of very porous material, and he obtained good agreement with the reflectance of a layer of lichens.

Hapke and Van Horn studied more than 200 surfaces, including a variety of rocks and minerals in both solid and powdered form, glass beads, metallic and nonmetallic whiskers, vegetation, such as grasses, lichens, and mosses, and artificial surfaces such as wires and sponges. Their experiments revealed that, in general, the reflectance law of a surface is determined by its albedo, the scattering characteristics of individual objects, and the structure in which these objects are arranged. They concluded that the upper layer of the lunar surface must be ". . . extremely porous and open with interconnected cavities and a void volume of the order of 90 percent. The scattering objects comprising the surface must absorb more than about 70 percent of the light incident on them and must be opaque, with fairly rough surfaces" [13, p. 4566]. Because of the need for interconnected cavities and the sharp backscatter peak, they exclude rocks, even those covered by cracks and pits, scoriaceous rock foams, slags, and glassy or other transparent or translucent objects. All materials found to scatter light like the moon are said to have a porous dendritic or reticulated structure. Materials found capable of forming the required structure include vegetation, whiskers, sponges, and finely divided powders. Experimental curves obtained by Hapke and Van Horn for various substances are shown in figures 4 and 5, along with the normalized scattering functions of a Lambertian surface and the lunar surface.

Prior to the work of Hapke and Van Horn (and the subsequent publication of fig. 5c), a serious criticism of the lunar dust model, strongly suggested by measurements from many different disciplines, was that the photometric behavior of loose powders could not be reconciled with that observed from the lunar surface. It was postulated that only a rigid and highly porous model having steep walls and sharp irregularities could satisfactorily match the lunar reflectance curve. However, as discovered by Hapke [13, p. 4563]:

> If a dielectric, such as a piece of rock, is pulvarized to a large average particle size, and the powder is poured or sifted onto a plate, the resulting macrostructure is not particularly complex; viewed under a microscope, the surface resembles a pile of gravel. But if the particles are smaller than a certain critical size, and if they are deposited in such a way as to insure that they fall individually and impact the surface at a low velocity . . . then the grains will build up fantastically complicated structures . . . under a stereoscopic microscope, porous hills are seen, out of which grow towers and branches, many of them interconnected with lacy bridges. These "fairy-castle" structures are fully as complex as the lichen and are certainly capable of sharply backscattering light.

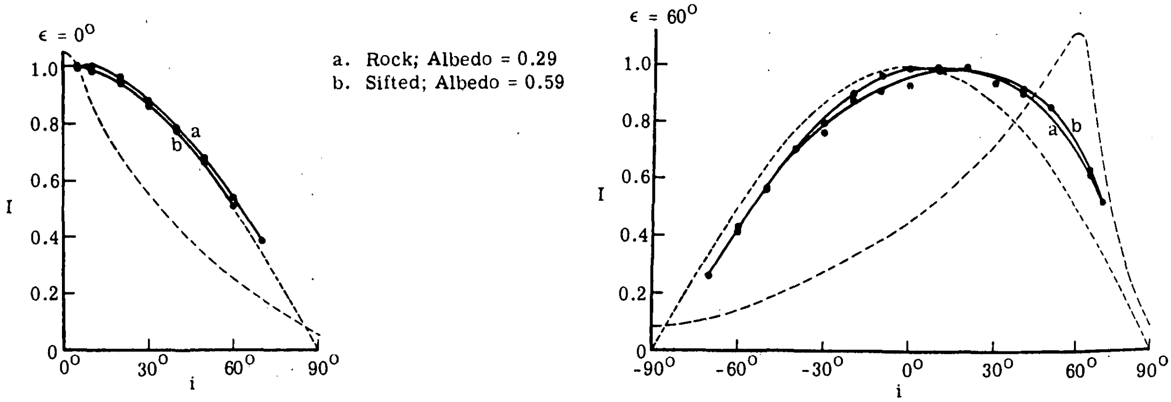

(a) Pumice

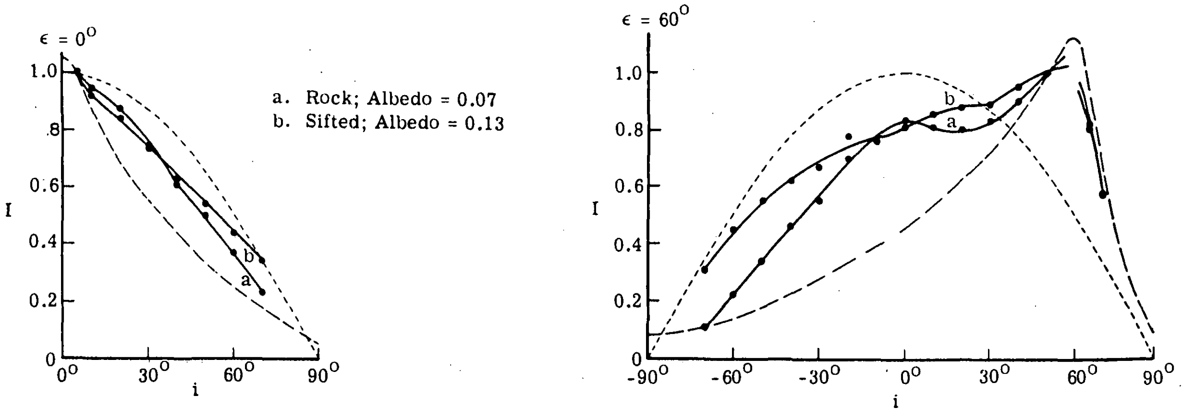

(b) Scoria

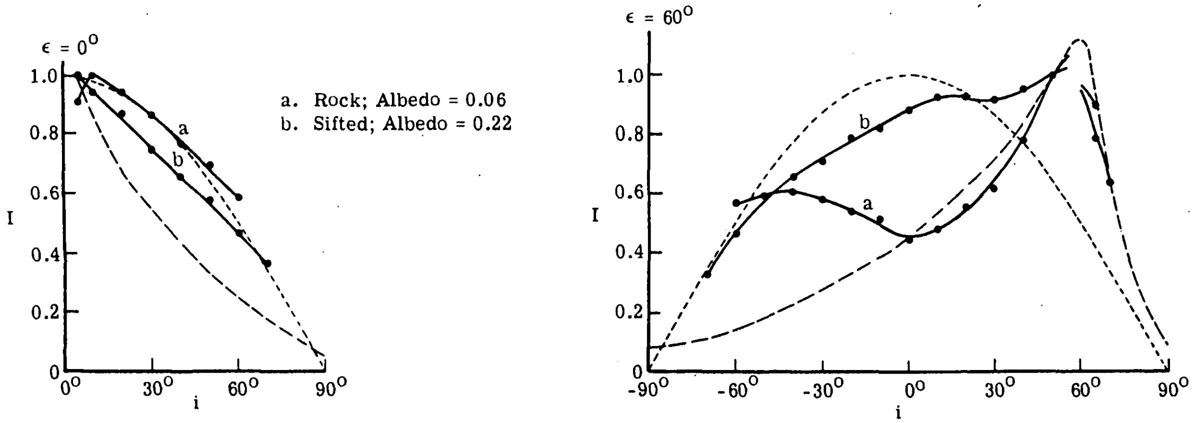

(c) Basalt

Figure 4. NORMALIZED SURFACE BRIGHTNESS VS. ANGLE OF INCIDENCE FOR VARIOUS TERRESTRIAL MATERIALS. ε = angle of observation. ----: Lambertian surface; - - -: lunar surface. [13]

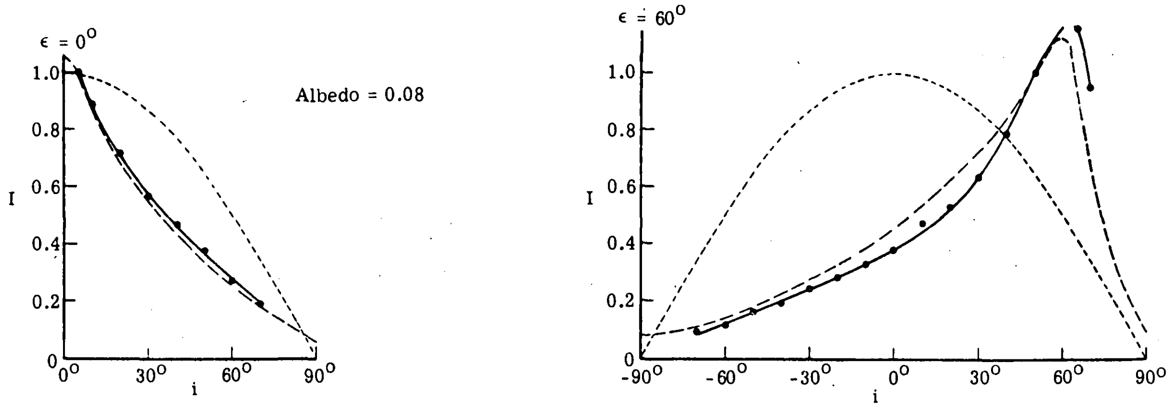

(a) Lichen

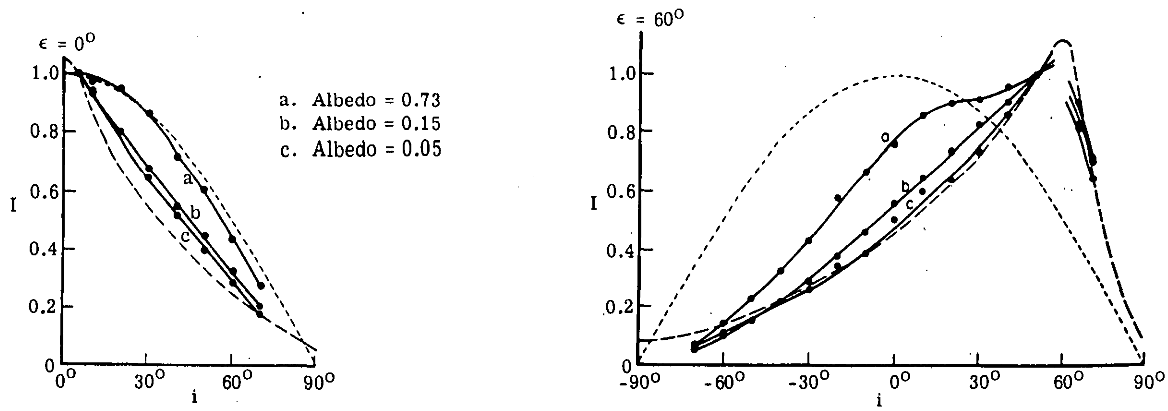

(b) Cellulose Sponge

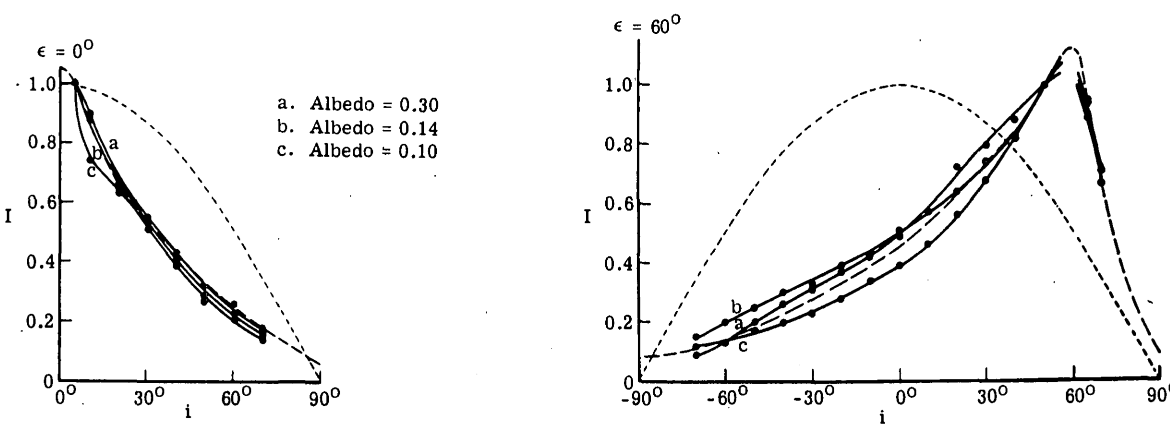

(c) AgCl Powder in Fairy-Castle Packing

FIGURE 5. NORMALIZED SURFACE BRIGHTNESS VS. ANGLE OF INCIDENCE FOR VARIOUS SUBSTANCES. ϵ = angle of observation. ----: Lambertian surface: - - - -: lunar surface. [13]

Hapke found that a subsequent exposure to ultraviolet radiation decreased the albedo (of powdered AgCl) and further sharpened the backscatter peak.

The ability to build complex, intricate structures is thought to be a property of all finely divided solids. Hapke concludes that it is "likely" that the structures responsible for the steep lunar backscatter are built into a form similar to his fairy castles over geologic times by the action of micrometeorite impacts and Gold's electrostatic transport mechanism [44]. The required low albedo could be derived from environmental effects such as high-energy cosmic radiation.

Enhanced backscatter from such a surface is explained by attenuation inherent in multiple reflections among the various interstices. Incident radiation is said to be reflected directly back (along the line of incidence) with little attenuation, while that reflected in any other direction is partially blocked and absorbed. Hapke was able to treat the reflection process from such a surface mathematically and derived a theoretical expression said to predict accurately the observed lunar photometric behavior.

The dendritic growth of Hapke's fairy castles and their near-lunar photometric function have been accepted as the solution by a great many workers, anxious for a "dusty" moon to account for other observed phenomena. However, as noted by Sharanov [18], it is necessary to consider the vast area of lunar terrain which contributes to an average brightness observation. As this area becomes larger, a greater degree of surface irregularity can contribute to an elongated reflection diagram. This will not be true in the case of the relatively minute laboratory specimens normally used for comparison. Sharanov suggests that terrestrial landscapes appear to be comparable in degree of elongation when viewed from sufficiently great distances, and states: "There is no need whatever to jump to conclusions about the existence on the moon of coverings resembling moss, grass, shrubbery, etc." [18, p. 747].

Adequate measurements of comparable photometric behavior are available to indicate that the complex situation postulated by Hapke and Gold, while possibly sufficient, is probably unnecessary. For example, Dobar [41] describes several simulated lunar materials exhibiting a comparable photometric function produced by exposing molten silica, basalt, and granite specimens to a vacuum. During upwelling, some of these materials have been observed to produce a color phenomenon similar to that reported by Greenacre during the 1963 Aristarchus events. Typical photometric curves appear in figure 6.

The lack of a known cohesive macrorough specimen satisfactorily duplicating the lunar reflectance curve is not sufficient proof that such does not exist, nor is it sufficient proof of the dust layer hypothesis. As noted by Sharanov and later by Halajian [42], the limitation may

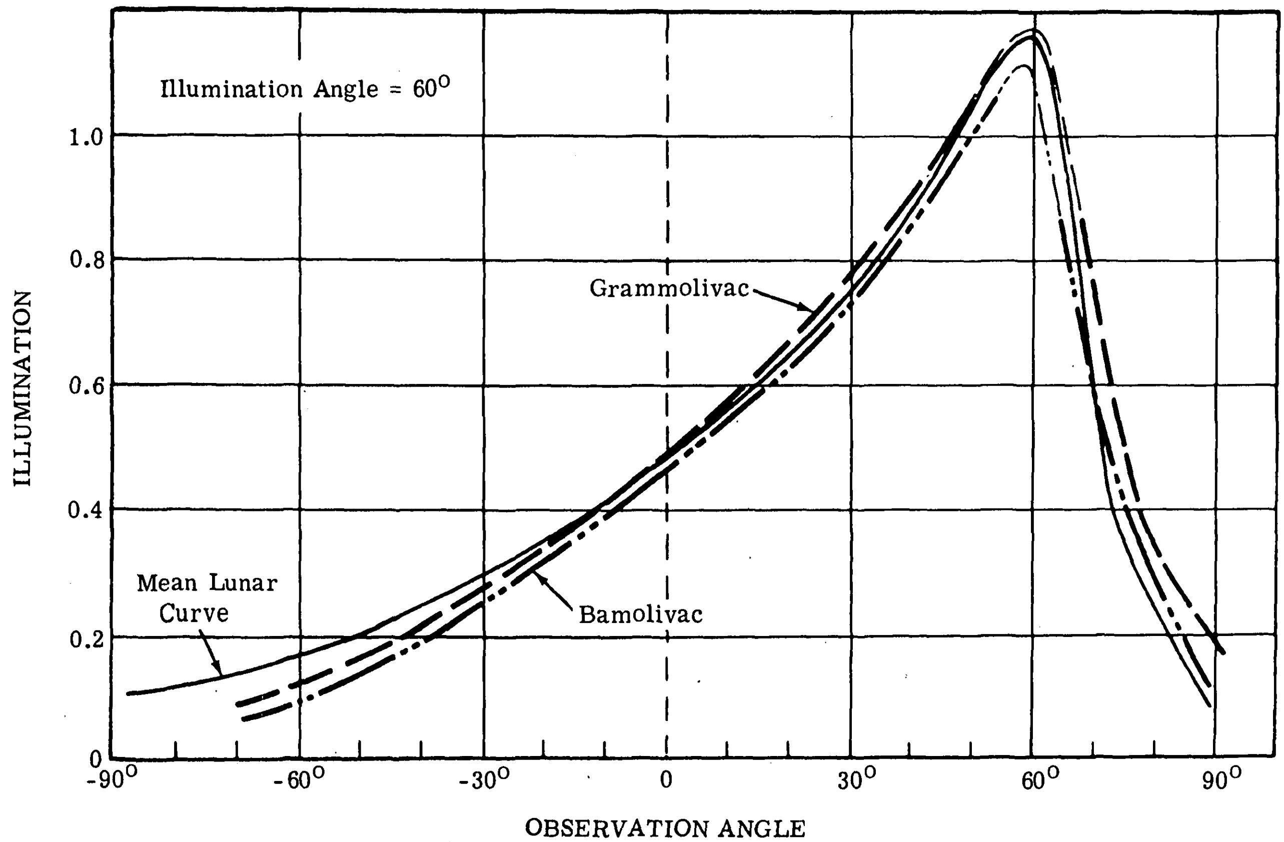

FIGURE 6. PHOTOMETRIC CURVES FOR THE MOON AND SIMULATED LUNAR MATERIALS [41]

well result from instrument limitations rather than from a lack of suitable terrestrial materials. Photometers (used by Hapke and others) typically examine spots no larger than 1/2 in. in diameter, while lunar measurements involve surfaces several orders of magnitude larger. Large-scale irregularities, universally rejected as unacceptable, may well duplicate the characteristic lunar backscatter if properly observed. In an attempt to verify this hypothesis, Halajian used a "large photometer" capable of investigating macroroughness over a 3-in. viewing area to examine various "specimens, other than fine dust, which reproduce the lunation curve as successfully as the metallic oxide powers of Hapke" [42, p. 674]. Specimens included a volcanic ash (strongly indicated by polarization measurements, but rejected by van Diggelen); porous slag (suggested by the albedo and color studies of various Russian observers but rejected by Hapke); block meteoritic specimens, dendrites, sponges, and sea coral. Halajian's data show that all these specimens exhibit a sharp backscatter, in some cases even exceeding the lunar surface. The photometer was calibrated by measuring Hapke fairy-castle powder as a reference. Curves obtained for particularly interesting materials are shown in figure 7,

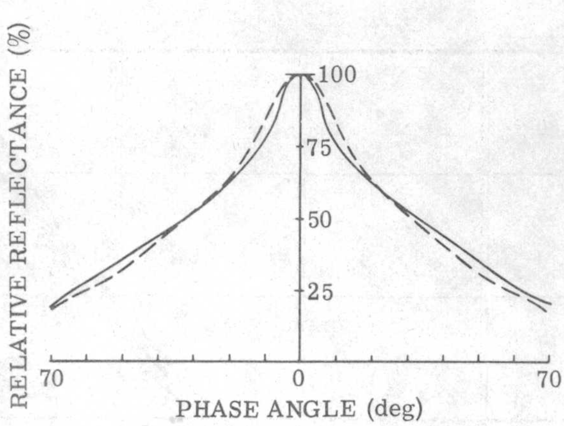

(a) AgCl Powder in Fairy-Castle Packing

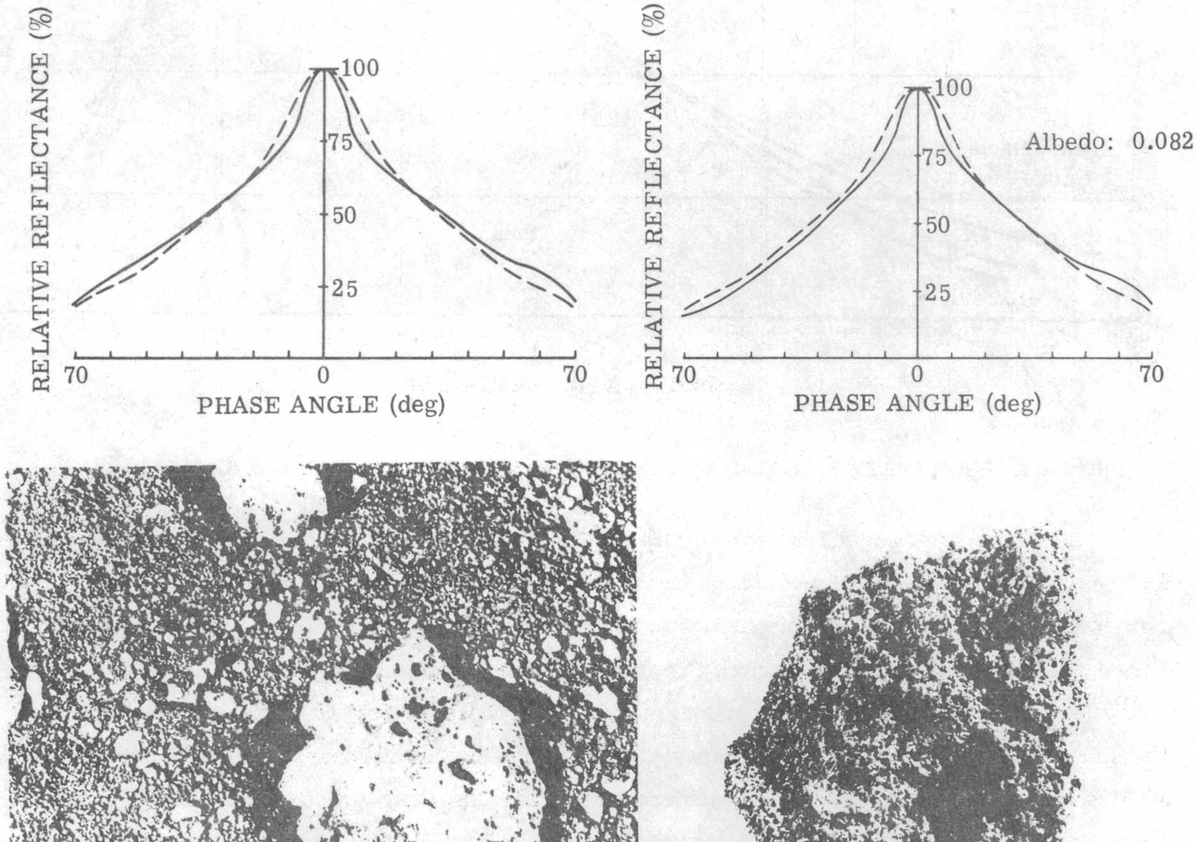

(b) Hawaiian Volcanic Ash

(c) Furnace Slag

FIGURE 7. REFLECTANCE CURVES OF COHESIVE TERRESTRIAL MATERIALS. Compared to lunar and fairy-castle photometric behavior. ___: sample; ----: lunar. [42]

compared to the standard lunation curve of Fedoretz [34] and AgCl in fairy-castle packing. Note the remarkably similar behavior of agglomerates, large blocks, and fine dust when viewed over a sufficiently large area. The volcanic-ash specimen is significant because of its inhomogeneity and its similarity to Surveyor I photographs of the surface of Oceanus Procellarum. Halajian concludes [42, p. 682]:

> . . . the surface complexity needed to backscatter light like the moon is not peculiar to fine dust, but could be equally reproduced by a macro-rough surface when measured by a large photometer. The volcanic ash and the furnace slag rejected by van Diggelen and Hapke, respectively, are examples of such surfaces.
>
> The differences in consistency, depth, scale of roughness, bearing strength and chemical composition between the good models indicate that any direct inference regarding these properties of the outermost layer of the moon on the basis of its photometry alone is premature and unjustified.

Nevertheless, in an otherwise excellent deduction of potential lunar surface characteristics from currently available data, Halajian rejects all solid rocks, packed soils, and much of the rock froth, slag, and cohesive material. These are said to be incompatible with the low bulk densities suggested by the photometric behavior of highly porous materials or fairy-castle packing of fine powders. In light of the above quotation and photometric data from cohesive porous materials, the reasons for this rejection are not clear.

It should be noted that, with the removal of this low-bulk density (high-porosity) requirement, a model of somewhat agglomerated, loosely packed soil, interspersed with varying sizes and amounts of bare rock, seems capable of satisfying the requirements of other measured parameters such as backscatter, polarization, albedo, color, and thermal variations. Such an interpretation, strengthened immeasurably by Surveyor I photographs, suggests a quite familiar barren and rock-strewn terrestrial field, perhaps differing only by a somewhat lower compaction and the exposure to a more severe radiation and particle bombardment.

Recent measurements on a wide variety of materials by Oetking [43] seem to fully confirm Halajian's suggestion that the problem of lunar reflection has resulted from instrument limitations rather than some peculiar composition or complex structure. Oetking's experiments indicate, contrary to the results of other investigators, that nearly all ordinary surfaces exhibit a pronounced rise in reflectivity near zero phase angle. He feels that this effect has been undetected because the instruments admitted light from too great a spread in phase angle (in the full-moon situation, all reflection is confined to a $1/2^{\circ}$ spread). In Oetking's instrument, the spread of light rays reaching the detector is held to less than $3/4^{\circ}$, while the detector can be adjusted to within 1° of zero phase. Reflectance data for various samples are compared to an ideal Lambertian surface and to the observed lunar surface in figures 8 and 9.

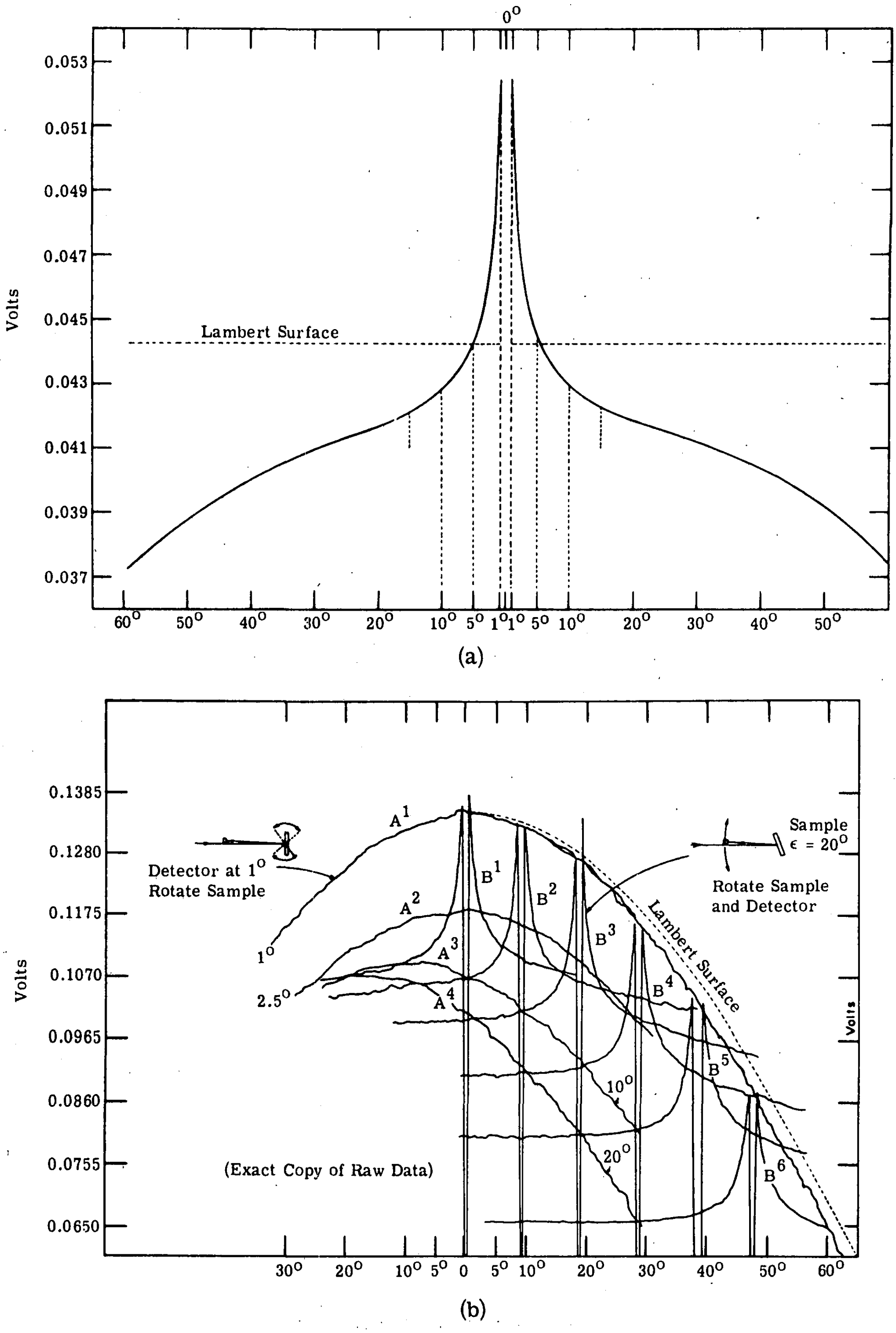

FIGURE 8. REFLECTIVITY OF MgO VS. ANGLE OF INCIDENCE. (a) Observation normal to face. (b) Curves B^1 through B^6: similar to (a) except that they are viewed in 10° increments to 50° from normal; curves A^1 through A^4: detector and source are separated by 1°, 2.5°, 10°, and 20°. [43]

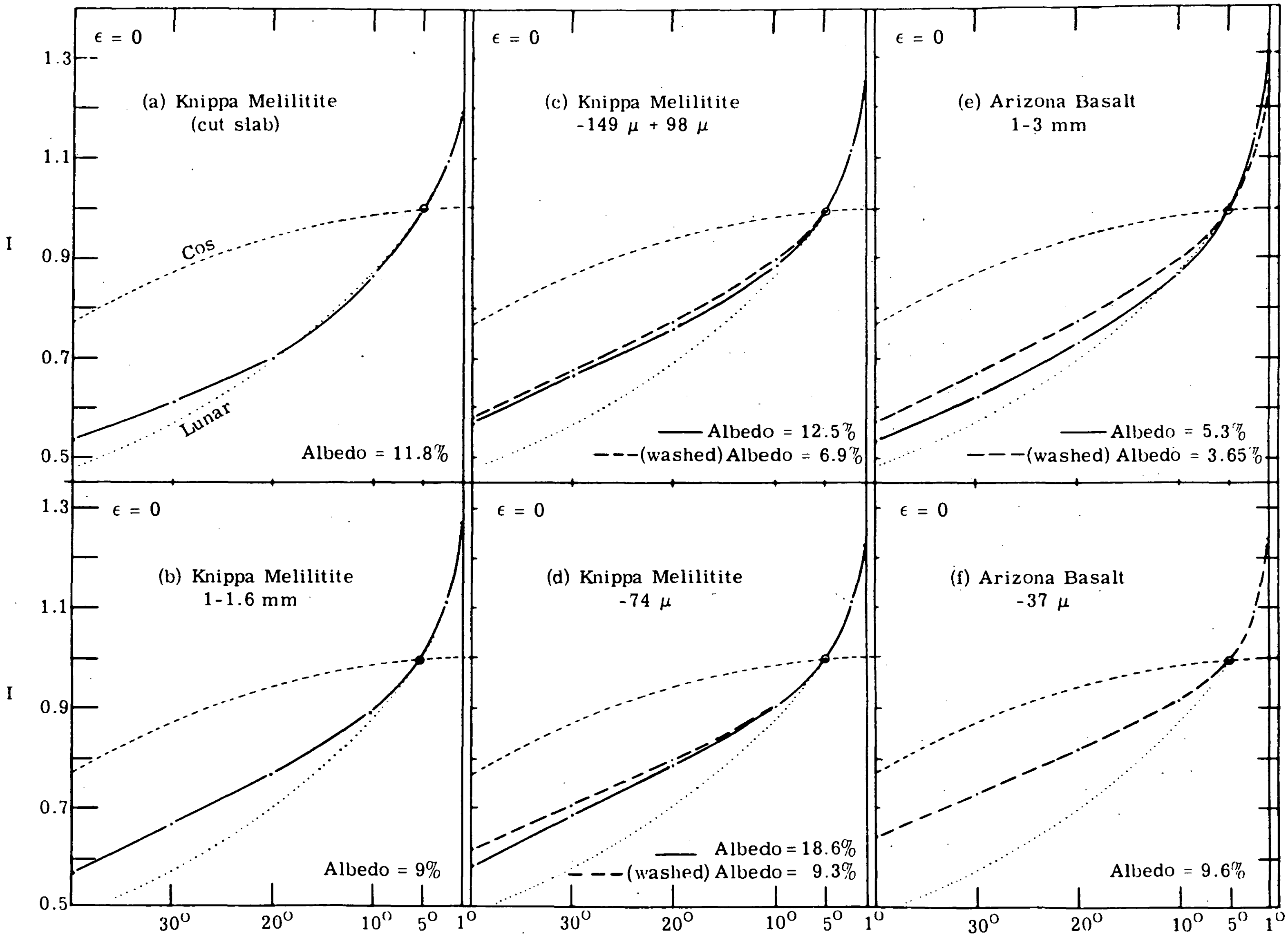

FIGURE 9. REFLECTIVITY CURVES OF VARIOUS MATERIALS [43], ----: cos i, ...: standard lunar photometric curve of Van Diggelen [33].

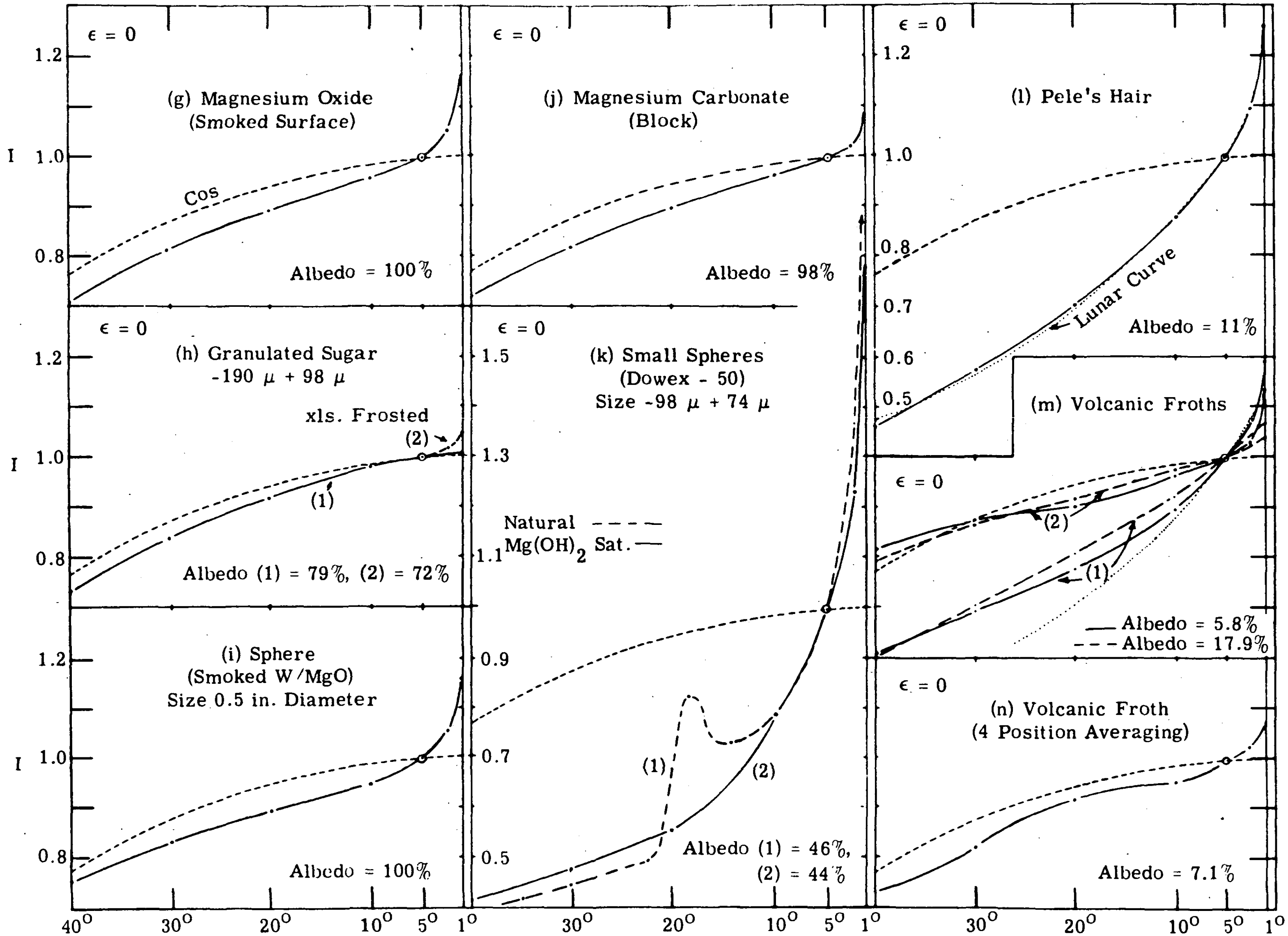

FIGURE 9. REFLECTIVITY CURVES OF VARIOUS MATERIALS [43]. ----: cos i; ····: standard lunar photometric curve of Van Diggelen [33]. (Continued).

Figure 8 consists of raw data illustrating the behavior of a heavily smoked MgO surface. Deviations from the ideal Lambertian surface at large angles of incidence confirm earlier measurements; however, in this case there is an appreciable difference at small angles as well. The curve of figure 8a is obtained by viewing normal to the surface as the angle of incidence is varied. Curves B^1 through B^6 of figure 8b are similar results, obtained for viewing angles increased in 10^o increments to 50^o from normal. Curves A^1 through A^4 were obtained by fixing the source and detector separation at angles of 1^o, 2.5^o, 10^o, and 20^o, respectively, as the sample was rotated. For the situation corresponding to figure 8a and the B curves of figure 8b, a Lambertian surface would have given a horizontal response (shown on fig. 8a only). Figure 8b shows that the maximum brightness always occurs near zero phase.

For the curves of figure 9, raw data have been multiplied by cos i to make them directly comparable to the lunar case. Figures 9a through 9f illustrate reflectance curves for different types of basic rocks in various stages of crushing, and suggest that the sharp backscatter peak is essentially independent of both particle size and albedo. In fact, the cut slab agrees best with the lunar surface; the remaining curves merely illustrate the diversity of textures and materials which exhibit a sharp backscatter peak near zero phase. Note in particular the remarkable similarity of the data of Pele's hair to the lunar curve (fig. 91).

These data have shown, surprisingly that the reflectivity of most terrestrial materials is characterized by a similar angular dependence, marked by a pronounced backscatter peak, and that a great many of these closely approximate the lunar reflectance curve. Hapke has confirmed Oetking's observations after appropriate modifications to his own instrument. He states, "I have become persuaded of the reality of the phenomenon . . . the brightness surge was readily observed on most surfaces" [45, p. 2515].

Myriad combinations and mixtures of particle size, depth, porosity, compaction, composition, albedo, shape, structure, and orientation can be called upon to account for local differences such as bright rays, certain craters, the maria, etc. Thus the work of Halajian and Oetking has removed much of the mystery surrounding the "peculiar" photometric behavior involving the full-moon brightness peak and absence of limb darkening. Simultaneously, it has added immeasurably to the confusion as to the composition and detailed structure of lunar surface materials. The photometric function alone can yield very little significant information concerning these important parameters. In particular, it should be noted that the universally accepted requirement of a highly porous (low-bulk density) surface layer must now be reconsidered.

5
LUNAR THERMAL MEASUREMENTS

At optical frequencies and into the near infrared (to perhaps 3 to 4 μ), lunar radiation is dominated by reflected solar illumination. At longer wavelengths, through the infrared and microwave portions of the spectrum, thermal emission predominates. As may be inferred from the uniformly low albedo, the energy content of emitted radiation appreciably exceeds that of the reflected portion. Measurements of the magnitude and variation of lunar emission are indicative not only of surface and subsurface temperatures but also of certain characteristics of lunar materials.

5.1. SURFACE TEMPERATURES IN THE INFRARED

The earliest measurement of lunar temperature was made by Lord Rosse in 1868 [46]. Using opposing thermopiles and a galvanometer, he measured the total light of the entire disk compared to that transmitted through a glass plate and deduced an effective full-moon temperature of 397°K. Rosse also determined a phase-angle relationship for total thermal radiation that agrees substantially with those of later investigators. Subsequent observations were made by Langley in 1884 [47] and Very in 1898 [48].

Few additional measurements were reported until the extensive work of Pettit and Nicholson in 1930 [49]. They measured the total heat radiation between the cutoff wavelengths of a glass window and a rock-salt window (about 5 to 20 μ), establishing a maximum observed temperature of 407°K (at the center of full moon) and a minimum of 120°K (center of the dark hemisphere). They also plotted the variation in observed temperature of the subsolar point with phase, finding that, although it reached a maximum of 407°K at full moon, it was only 358°K at quarter phase (see fig. 10). The temperature of a Lambertian surface which would give the same total radiation was found to be 391°K.

Sinton [50, 51] used a narrowband filter at 8.8 μ to determine a midnight temperature of 122 ± 3°K, in close agreement with that of Pettit and Nicholson (120 ± 5°K). He also determined a non-Lambertian variation in heat emitted by the subsolar point as a function of phase which closely parallelled, although slightly lower, that formerly determined (see fig. 10). Sinton obtained a mean spherically emitting surface temperature of 389°K (1.75 cal-cm^{-2}-min^{-1}).

Despite the close agreement in the antisolar-point temperatures reported by Pettit and Nicholson and by Sinton (as a result of quite different measurement techniques), it has been pointed out by Saari [52] that the former is probably in error. The existence of an atmospheric window beyond 16 μ discovered by Adel in 1959 [53] was unknown to Pettit and Nicholson and this radiation was not included in their calculations. Saari suggests a correction downward to about 108°K, based upon the atmospheric emission data of Bolle [54].

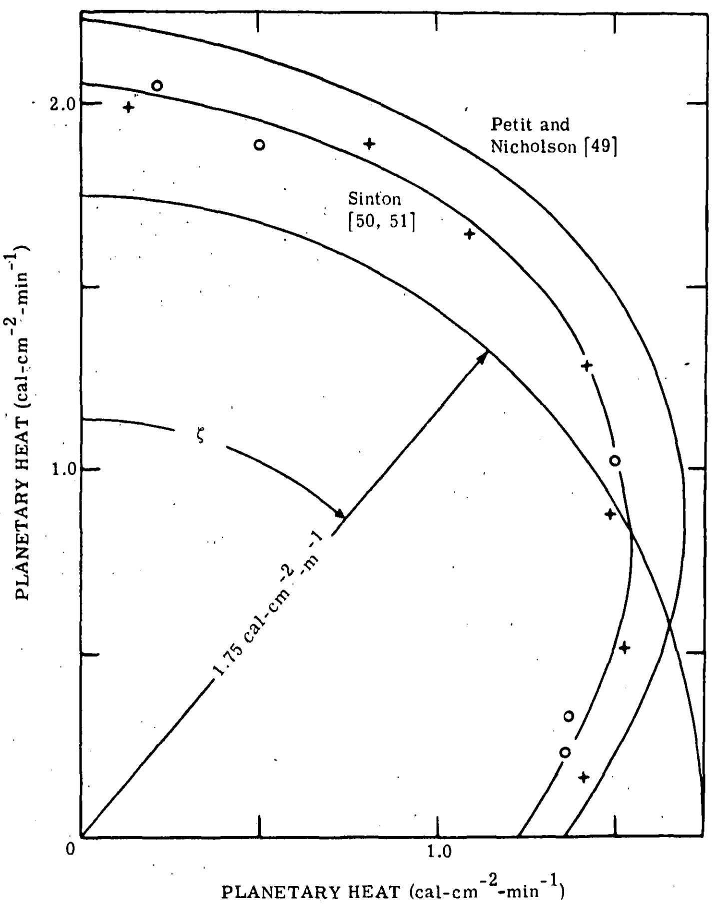

FIGURE 10. HEAT EMISSION OF SUBSOLAR POINT OF MOON. Heat emitted by the subsolar point of the moon is shown as a function of the angle ζ from the normal to the surface. +: before full moon; 0: after full moon. [50]

Recent measurements by Murray and Wildey [55] and by Shorthill and Saari [56] substantiate Saari's contention that the midnight temperature may be well below the previously accepted 120°K. Data from these measurements are shown in figure 11, from which Saari obtained, through extrapolation, antisolar-point temperatures of approximately 106°K [55] and 99°K [56]. He suggests that these values be combined with his modified value for the Pettit and Nicholson data to yield an average midnight temperature of 104°K. Evidence of an even lower minimum lunar temperature is obtained from the fact that, while the measurements of Murray and Wildey were low-frequency noise limited to a minimum detectable temperature of 105°K, they indicate that actual nighttime temperatures fell below this value [55, p. 744].

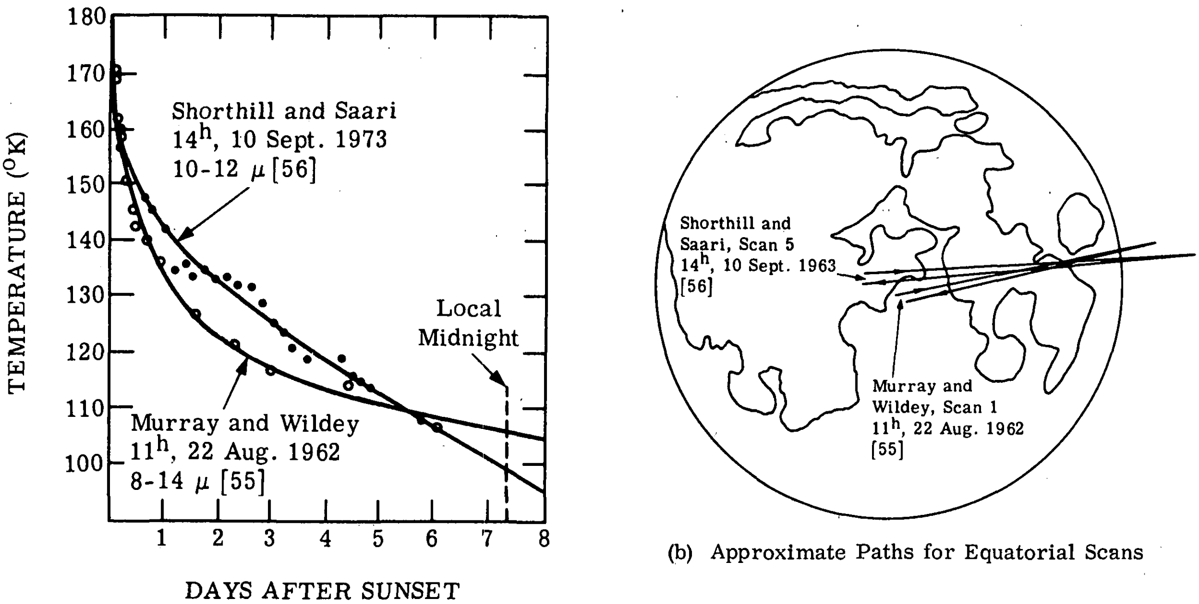

(a) Dark-Side Temperatures Obtained from Equatorial Scans

(b) Approximate Paths for Equatorial Scans

FIGURE 11. DARK-SIDE THERMAL SCANS OF MOON [52]

In 1964, Low [57] measured an upper limit for the minimum nighttime temperature of less than 100°K in the 7.5- to 13.5-μ band. In 1965, he reported scans across the cold limb in the 17.5- to 22-μ window [58]. These latter data, taken at various places over the disk, indicated a mean temperature of 90°K, but included individual nighttime values from less than 70°K to greater than 150°K.

Thus, as an improving technology allows more sensitive and precise measurements, the upper limit of minimum lunar nighttime temperatures is continually decreased. Further improvement, particularly in spatial resolution, will almost certainly yield still lower values. Previous earth-based observations have utilized relatively coarse resolution [e.g., Murray and Wildey, 26 arcsec (~48 km); Shorthill and Saari, 8 arcsec (~15 km); Low (1964), 15 arsec (~28 km); Low (1965), 18 arcsec (~34 km)]. Temperature measurements averaged over such large surface areas can obviously include a wide range of structural and compositional effects, such as emissivity-wavelength variations or unique angular-emission behavior. Such circumstances are often postulated to explain anomalous behavior but at present are purely speculative.

For example, the two curves of figure 11a differ appreciably in both individual data points and general shape. This is not too surprising since the corresponding scans covered similar, but not identical, areas (see fig. 11b), using different spectral bandwidths (10 to 12 μ and 8 to 14 μ) and different spatial resolutions (15 km and 32 km). Despite basic observational differences, the two measurements agree around 4 to 5 days after sunset, where the scans crossed a common area; this fact strongly favors structural or compositional effects as a cause of variations at different positions around the disk.

It should be explicitly noted that such temperature measurements are not, strictly speaking, lunation measurements since they do not involve the observation of a given position on the lunar disk as a function of phase angle. Rather, they are the result of nearly simultaneous measurements obtained through drift curves or (as in this case) right ascension scans across the lunar disk at a given phase. (They are referred to later in this report as lunation measurements to distinguish them from eclipse measurements.) Such an observation must inherently include the effect of any local variations or an unknown angular-emission behavior.

5.2. MICROWAVE MEASUREMENTS OF SUBSURFACE TEMPERATURES

Data obtained in optical frequency observations are governed entirely by surface phenomena such as the reflection of solar illumination. Infrared observations, on the other hand, while measuring surface temperatures (or those at very shallow depths), are directly dependent upon the physical and thermal characteristics of subsurface material. However, the determination of surface parameters alone leaves an appreciable ambiguity as to the nature of subsurface characteristics affecting the measurement.

Surfaces such as the outermost layer of the moon which are opaque at optical frequencies, and perhaps only very slightly transparent in the infrared, become considerably more transparent to microwave radiation. Thus, long-wavelength observations can potentially yield an insight into subsurface phenomena to a depth of at least a wavelength and possibly to several wavelengths [59].

Of the many limitations in the measurement of microwave radiation from the moon, one of the foremost has been attainable resolution. Because of the long wavelengths involved, measurements result in a weighted average over several thousand square kilometers, in many cases the complete disk.

The first observation of lunar thermal radiation at microwave frequencies consisted of a single measurement, at 1.25 cm, by Dicke and Beringer in 1946 [60]. The first extensive measurements were made by Piddington and Minnett [61], also at 1.25 cm, in 1949. Using an antenna beamwidth which averaged over most of the disk, they found the brightness temperature to vary almost sinusoidally as a function of phase angle along the equator. Assuming a uniform emissivity of 0.9, they determined a mean brightness temperature of $249 \pm 13^{\circ}$K, with a first-harmonic amplitude (variation throughout the month) of 52°K. The sinusoidal variation thus corresponds to temperature extremes a few centimeters below the surface of 197°K and 301°K compared to the currently accepted surface temperature extremes of about $90^{0}K$ and $400^{0}K$. This variation was found to lag the lunar phase angle by 45^{0}.

Many measurements have since been made, scattered irregularly through the microwave window, from wavelengths of 1.2 mm to near 1 m. Table III summarizes these data, compiled from various partial tabulations or individual reports.

TABLE III. MICROWAVE TEMPERATURE MEASUREMENTS

	Investigator	Wavelength (cm)	Mean Temp. (^{o}K)	Amplitude of Variation (^{o}K)	Phase Lag (deg)	Date	Ref.
1.	Low	0.12	222	65		1964	57
2.	Low and Davidson	0.12	229	——		1965	62, 63
3.	Fedoseyev	0.13	219	121	16	1963	63
4.	Admenitsky	0.15	250	100			64
5.	Sinton	0.15	228	108	——	1955	50, 65
6.	Gary et al.	0.33	196	——	——	1965	59
7.	Kislyakov and Salomonovich	0.4	228	86	27	1963	63
8.	Salomonovich	0.8	197	32	40	1958	50, 64
9.	Salomonovich and Losovsky	0.8	211	40	30	1962	63
10.	Gibson	0.86	180	30	39	1958	50, 64
11.	Piddington and Minnett	1.25	249	52	45	1949	50, 61
12.	Zelinskaya	1.63	224	36	——	——	64
13.	Grebenkamper	2.2	200	15	——	——	64
14.	Troitskii and Zelinskaya	3.2	170	<12	——	1955	50
15.	Kaschenko et al.	3.2	223	17	45	1961	63
16.	Mayer et al.	3.2	195	12	44	1961	63
17.	Cook et al.	3.45	221	——	——	1961	66
18.	Akabane	10	315	36	45	1955	50,64
19.	Mezger and Strosol	20.5	250	<5	——	1959	50
20.	Westerhout	21	170	0	——	——	64
21.	Denisse and LaRoux	33	189	19	——	——	64
22.	Seeger et al.	75	185	<18	——	1957	50
23.	Seeger	75	186	0	——	——	64

Many analysts of these data have sought to establish a trend, to infer the depth of penetration of the thermal wave, and to determine mean values and limits for an invariant subsurface temperature. The resulting interpretations vary as appreciably as do the individual data points. For example, Krotikov and Troitskii [63, 67] have plotted certain of the available measurements (the darkened circles of fig. 12a) and deduced a thermal gradient increasing with depth below the lunar surface. They interpret this gradient to indicate a radioactive heat flux 4 to 6 times that previously predicted for a chondritic lunar material [62, p. 4].

In order to compare the data used by Krotikov and Troitskii to infer a thermal gradient with other available data, a more complete set of measurements is plotted in figure 12a (including the Krotikov and Troitskii data). It is obvious that the increase with depth apparent in the limited data they considered is lost in the scatter if all available measurements are included. Since no trend is apparent from the data of figure 12, all mean brightness temperatures have simply been averaged to yield the dotted line at $224^{\circ}K$. This value seems as likely as any other to correctly represent an invariant subsurface temperature. It is interesting to note that Troitskii has reported elsewhere a constant $-50^{\circ}C$ ($223^{\circ}K$) at a depth of 0.5 m [68] and that Kopal arrives at the same value from the data of Denisse and LaRoux [9, 69]. He expects the penetration to reach "barely half a yard below the surface" [70, p. xvi].

To gain some insight into the depth of penetration of the diurnal heat wave, the amplitude of variation given for measurements of figure 12a has been plotted in figure 12b. The dashed curve has no statistical significance beyond indicating a general trend. Although the data also exhibit considerable scatter, variations appear to become negligible at a wavelength slightly less than 1 m (although not necessarily at depths of less than 1 m). While it has been postulated that microwave radiation arises from depths as great as several wavelengths, contributions from all lesser depths are included in a given measurement; these contributions cause, in part, the observed amplitude variation. Thus an average depth on the order of one wavelength and a diurnal heat wave penetration on the order of 1/2 to 1 m seem realistic.

Russell [71] has analyzed a homogeneous semi-infinite solid with specified periodic boundary temperatures derived from the infrared lunation measurements of Sinton [50] (unfortunately, these include his midnight temperature of $120^{\circ}K$). He determined a constant temperature of $229^{\circ}K$ at a depth of 20 cm, equivalent to the average value of surface temperature over one period.

On the earth, a diurnal heat wave more than an order of magnitude smaller in amplitude and acting over a period only 1/30 as long penetrates to approximately the same depth [72, p. 31, 74]. Thus, whatever the exact nature of lunar surface and subsurface materials, it is clear

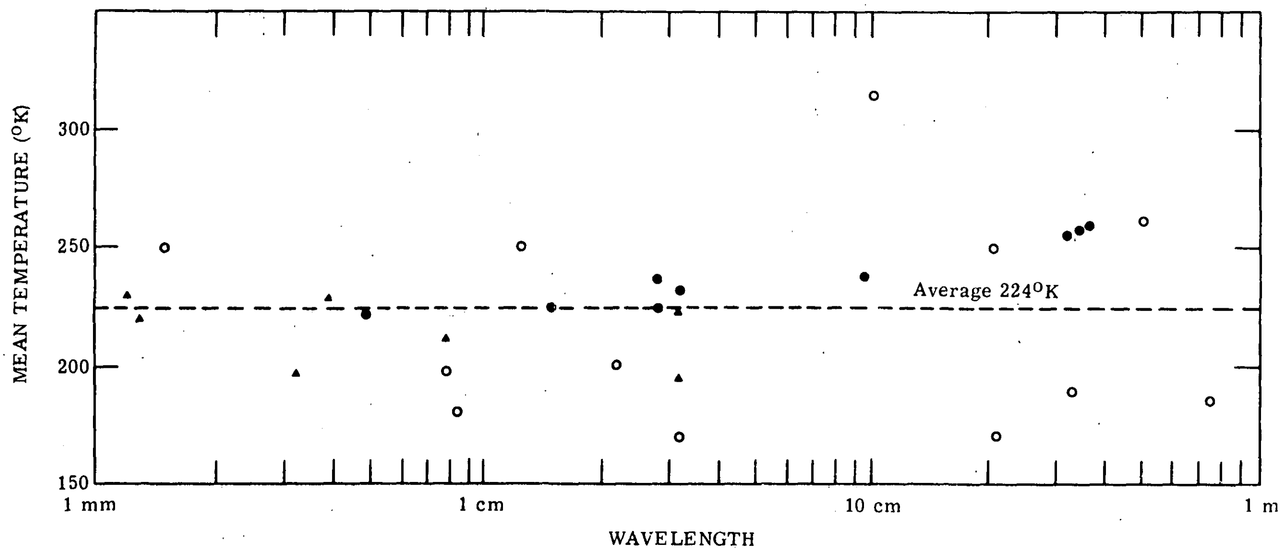

(a) Observed Values of Mean Component of Lunar Brightness Temperature vs. Wavelength

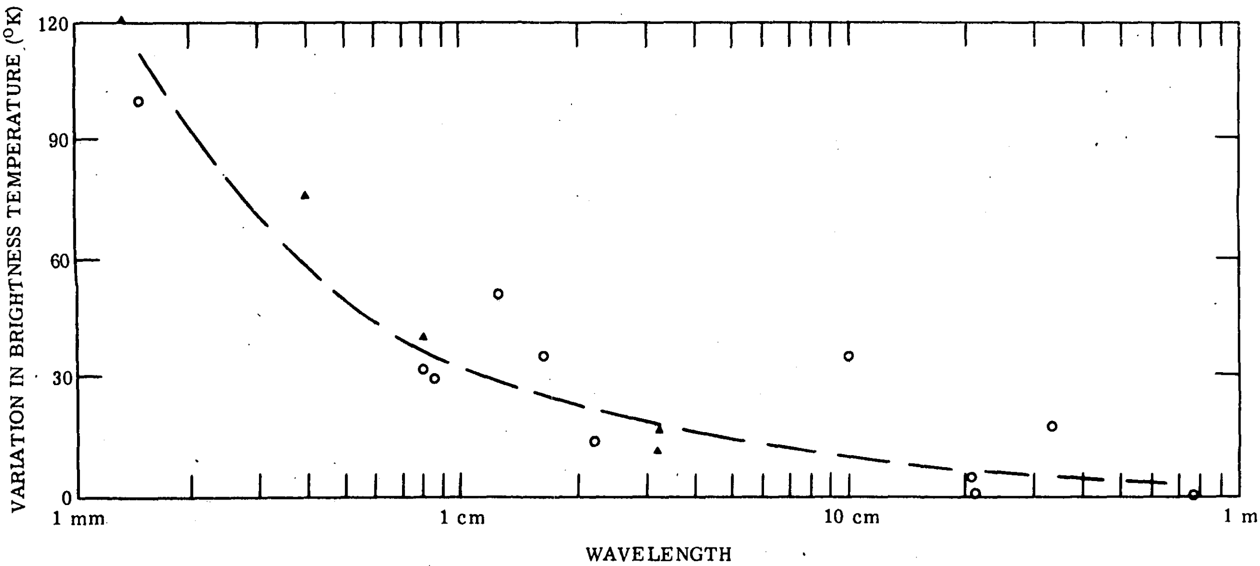

(b) Amplitude of Lunation Variation in Brightness Temperature vs. Wavelength

FIGURE 12. MICROWAVE BRIGHTNESS TEMPERATURE VS. WAVELENGTH. ▲ : after Linsky [63, table II]; ○ : after Jones [64, table II]; ● : after Linsky [63, fig. 2].

that their thermal inertia, or resistance to temperature change, $(K\rho c)^{-1/2}$, is very high. Here K, ρ, and c are the thermal conductivity, density, and specific heat of the material. In most early analyses of the moon, these have been assumed to be independent of both temperature and depth.

From infrared lunation measurements involving a midnight temperature of 120°K, Sinton [50] calculated $(K\rho c)^{-1/2} = 435$ cm^2-deg-sec$^{1/2}$, compared to a value of about 20 for most terrestrial rocks. It should be noted however, that this calculation is extremely sensitive to minimum lunar temperatures which, due to recent measurements, are continually being revised downward. As will be seen later, the currently accepted value of 90°K indicates an even higher thermal inertia (lower thermal conductivity) near 1200 cm^2-deg-sec$^{1/2}$.

Most investigators have interpreted laboratory measurements of the thermal conductivity and thermal inertia of terrestrial materials to indicate a lunar dust layer, extending at least to depths of significance to the microwave measurements. The various aspects of this interpretation are discussed more fully in the next section.

5.3. TEMPERATURE VARIATIONS DURING AN ECLIPSE

The diurnal thermal wave resulting from the periodic day-night insolation accompanying the moon's orbital motion is characterized by a period of just over 29 1/2 days, the synodic month. A similar thermal wave crosses the lunar disk, in the time span of an hour rather than days, during an eclipse.

Measurements of the rapid fall in lunar temperatures during an eclipse have been observed in both the infrared and very high frequency microwave regions of the spectrum. In the latter, it should be noted that variations are detected to wavelengths of only a millimeter or so, indicating that the eclipse-induced thermal wave barely penetrates the outermost surface layer. (Specifically, Piddington and Minnett [61] and Gibson [73] report no detectable change at wavelengths of 1.25 cm and 8.6 mm, respectively.)

Infrared measurements of the fall in temperature during an eclipse made by Pettit and Nicholson [49] in 1927 were used by Epstein [74] to deduce that the lunar surface was composed of a material whose thermal properties were similar to pumice. He assumed that the surface loses heat according to the fourth power of its initial (rather than actual) temperature and erroneously deduced a value of $(K\rho c)^{-1/2} = 120$. Wesselink [75] studied a more accurate nonlinear situation, using actual temperatures, and obtained a value of $(K\rho c)^{-1/2} = 920$, which he felt to be consistent with dust at low pressures.

Jaeger [76], Jaeger and Harper [77], and Lettau [78] independently confirmed Wesselink's calculations and established a value of $(K\rho c)^{-1/2}$ on the order of 1000, based upon the data of Pettit and Nicholson and of Pettit [79] for the 1939 eclipse. Similar values were obtained by Jaeger [80] from microwave observations of Piddington and Minnett [61]. All observers again attributed the high value to a layer of dust. Curve I of figure 13 represents the theoretical temperature variation for such a homogeneous surface layer having $(K\rho c)^{-1/2} = 1030$. The dots show Pettit's observation for the 1939 eclipse. The greatest disagreement occurs in the umbral phase, where observations indicate a lower temperature at the beginning of totality and a more gradual drop thereafter. As noted by Jaeger and Harper, this discrepancy will not be removed by changes in the value of $(K\rho c)^{-1/2}$ for a homogeneous material, which merely shifts the entire umbral portion (or the new-moon phase for a lunation) of the curve vertically (see fig. 14).

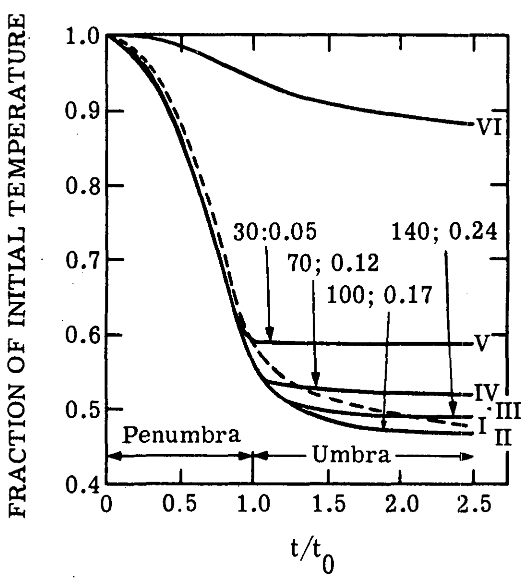

FIGURE 13. CALCULATED AND OBSERVED ECLIPSE COOLING CURVES [77]

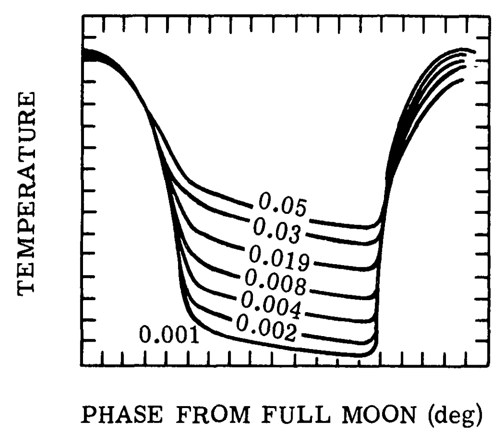

FIGURE 14. THEORETICAL TEMPERATURE VARIATION FOR HOMOGENEOUS MODEL [50]

In an attempt to resolve the difficulty experienced during the umbral phase, Jaeger and Harper suggested that the thermal inertia may vary with either temperature or depth. Being unable to reproduce the experimental data with what they considered "likely" temperature variations, they concentrated upon a variation with depth. Curves II, III, IV, and V of figure 13 are their curves for a two-layer model consisting of a thin dust layer with $(K\rho c)^{-1/2} = 1030$ over a more conductive substrate. The curves represent cases for a substrate $(K\rho c)^{-1/2}$ of 140, 100, 70, and 30 covered by a dust layer 0.24, 0.17, 0.12, and 0.05 cm thick, as shown on the figure. Curve III gives the best fit to Pettit's experimental data; the substrate corresponds to the value for terrestrial pumice or gravel. Curve VI illustrates the behavior of bare rock with $(K\rho c)^{-1/2} = 20$.

Jaeger interpreted the data to preclude the possibility of a lunar surface characterized by an extensive coverage of bare rock. He noted, however, that the spatial averaging involved in the observed temperatures could allow a small portion (possibly 5%) of bare rock with the remainder being dust. Fremlin [81] extended this argument and has suggested that rather than an inhomogeneity with depth, a surface mixture of bare rock and dust could give an "almost exact" fit with Pettit's observations. His model consists of bare rock of $(K\rho c)^{-1/2} = 20$ covering 4.8% of the surface and a dust of $(K\rho c)^{-1/2} = 2700$ covering the remainder. As he noted, the percentages and thermal inertias are quite arbitrary, being only one of probably several combinations which could be fitted to a given observation.

Murray and Wildey [55] have averaged data from their right ascension scans across the darkened disk (one of which is shown in fig. 11) and compared the average cooling curve to the homogeneous model of Jaeger (see fig. 15). While there is substantial disagreement, especially near the terminator, the general shape and cooling rate for the theoretical lunation cooling curves more closely approximate experimental data than do those for the eclipse cooling case. However, Murray and Wildey conclude that ". . . none of the curves fits at all well . . . a homogeneous layer of porous dust of centimeters to meters thickness is clearly ruled out" [55, p. 747]. As an alternative model, they suggest a horizontal conductivity variation and conclude that a significant amount of porous dust can exist only if it is mixed with bare consolidated rocks.

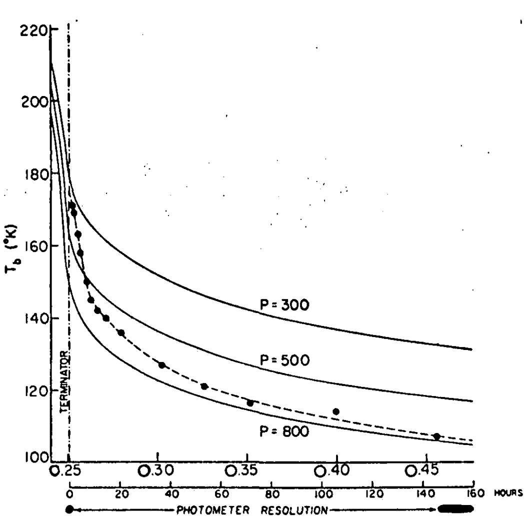

FIGURE 15. CALCULATED AND OBSERVED LUNATION COOLING CURVES. The observations have been averaged and plotted (•) as a function of time since passage of terminator. Also shown are calculated lunation cooling curves for an arbitrarily thick surface layer of $(K\rho c)^{1/2}$ of 300, 500, and 800. The calculations are after Jaeger [80] but are considerably more precise than those in his paper. An albedo of 20% was assumed. The thermal properties were assumed to be independent of temperature in Jaeger's analysis. [55]

Saari and Shorthill [82] obtained cooling curves for the craters Aristarchus, Copernicus, and Kepler and their environs during the eclipse of September 1960. Cooling curves for Aristarchus and its environs are shown in figure 16, where experimental data are compared to the theoretical curves of Jaeger for both a single-layer, homogeneous model and a two-layer model. While there is considerable scatter in the data (shaded areas), the agreement is considerably better with a two-layer model. (The fact that the crater cooled more slowly will be discussed later.)

The failure of all models to accurately represent more than one, or at best a few, isolated observations has stimulated a search by many investigators for an improved model. One of the lesser modifications (but resulting in a substantial improvement) is the one-layer calculation of Krotikov and Shchuko [83], similar to that of Jaeger but employing a more accurate, computerized iterative procedure and a different value of the solar constant. They used the more generally accepted value of 0.033 cal-cm^{-2}-sec^{-1} rather than the 0.0258 used by Jaeger. Their cooling curves are compared to Jaeger's in figure 17. It is evident that the slope of the new-moon (or umbral, in the case of an eclipse) portion is not improved and the total temperature drop at sunrise is only very slightly affected. However, a criticism of Jaeger's analysis, his failure to correctly represent the initial descent and sharp break at the beginning of total darkness, is substantially removed. Since this was a prime stimulus in his consideration of the two-layer model as opposed to his earlier homogeneous one-layer model, the result is significant.

Krotikov and Troitskii [67] have attempted to reconcile infrared and microwave measurements of brightness temperature and temperature variations with a one-layer model having a mean value of $(K\rho c)^{-1/2} = 350 \pm 70$. Since their analysis is frequently referenced by other workers in discussions of various observations, it should be noted that it is based upon several questionable assumptions. First, the range $300 < (K\rho c)^{-1/2} < 400$ is established as consistent with an antisolar-point temperature of 125°K. Temperatures in this range were reported by Pettit and Nicholson [49] and by Sinton [51], but are no longer generally accepted. In section 5.1 it was noted that recent measurements indicate a reduction in this figure by as much as 25%. The curves of figure 16 indicate an antisolar-point temperature of <100°K, which is consistent only with values of $(K\rho c)^{-1/2}$ greater than 1000.

Their next assumption is that the average radio brightness temperature is consistent with this range of $(K\rho c)^{-1/2}$. While this is true, the scatter associated with currently available data on this parameter (see fig. 12a) make the average value subject to a rather large error, greatly affecting the associated $(K\rho c)^{-1/2}$. Linsky [63] points out that a 5% error in measured temperature could change the deduced $(K\rho c)^{-1/2}$ by 300%. He states: "the value of $(K\rho c)^{-1/2} = 350 \pm 20\%$ as given by Krotikov and Troitskii is based upon a dubious infrared measurement, an abso-

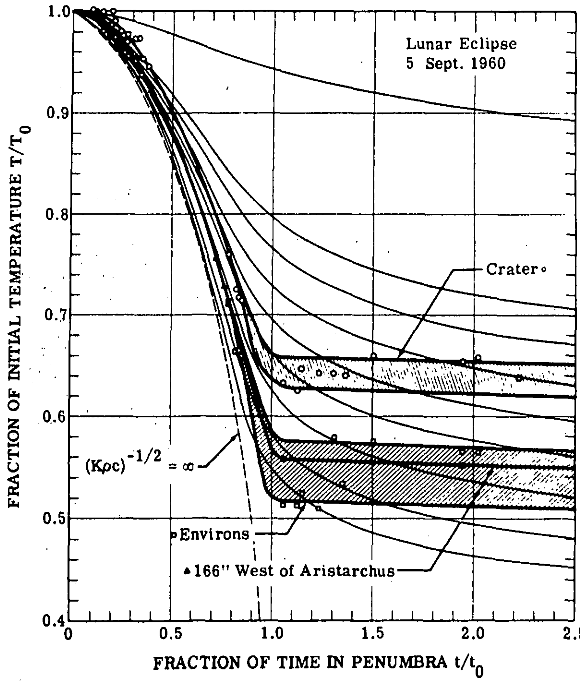

(a) Experimental Data and Theoretical Curves for Jaeger's Homogeneous Surfaces

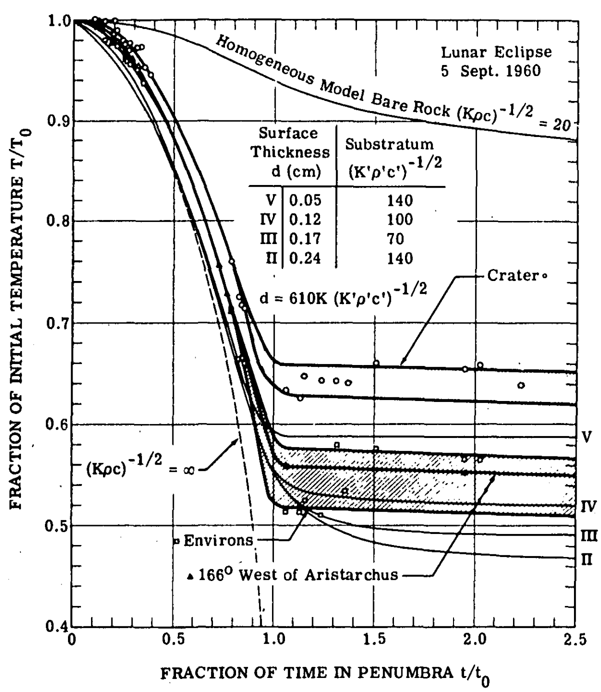

(b) Two-Layer Model [80]

FIGURE 16. NORMALIZED COOLING CURVES FOR ARISTARCHUS AND ENVIRONS [82]

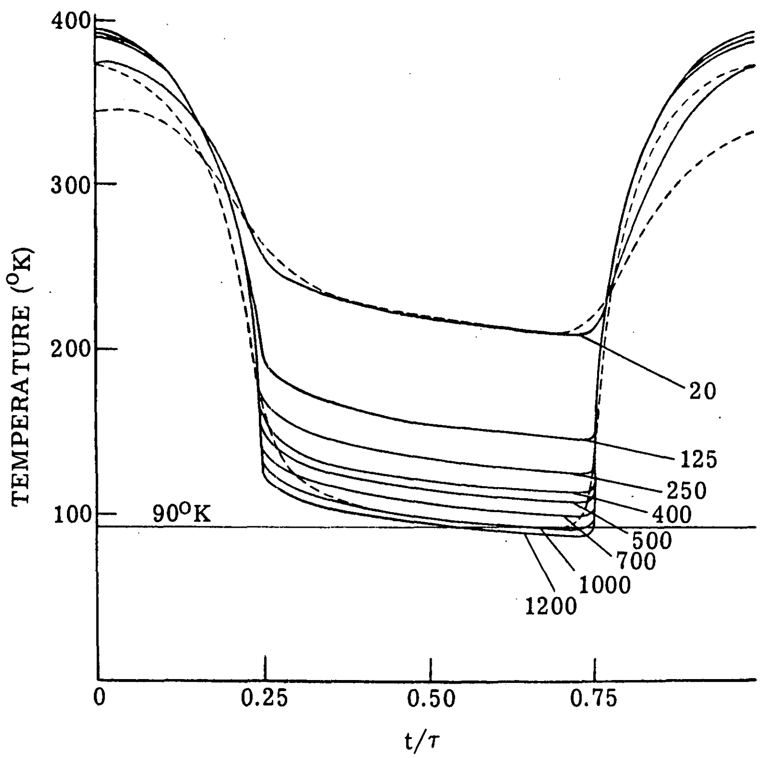

FIGURE 17. THEORETICAL TEMPERATURE VARIATIONS FOR HOMOGENEOUS MODEL. Broken lines are Jaeger's curves [80] for values of $(K\rho c)^{-1/2}$ of 20 and 1000. [83]

lute radio brightness temperature for which small errors greatly affect the conclusions and an extrapolation procedure that gives ambiguous results" [63]. Regardless of the details of the various arguments and interpretations of often conflicting and ambiguous data, it is unlikely that such a low value of $(K\rho c)^{-1/2}$ will be widely accepted.

Gibson [84] has proposed a complex three-layer model based upon observations at 8.6 mm. The upper layer, about 1/2 cm of a material resembling sand, overlays several centimeters of a material of high electric conductivity. Below these is a layer resembling rock to an undetermined depth. However, based upon observations at 4 mm, Kislyakov [85] proposes a mono-layer model.

Thus, there is a surplus of temperature-independent models designed for the most part to account for a single set of observations, often to the exclusion of other, equally reliable observations. The assumption of temperature-independent thermal properties is common to all models discussed so far. Both Wesselink and Jaeger realized the limitations imposed by this assumption but were unable to satisfactorily include a temperature dependence in their calculations. Lucks et al. [86] considered this problem in 1951, and measured both K and c as a function of temperature for fused quartz and various metals and plastics. Later, Muncey [87] concluded that both K and c could exhibit a temperature dependence such that $(K\rho c)^{-1/2}$ would be near 300 at 300°K. Tyler and Copeland [88] developed a homogeneous model including such temperatures in 1962, and recently Linsky [63] has studied this possibility extensively. Linsky developed eight models, six having temperature-dependent parameters as well as allowing for a radiative component of heat transfer. The radiative component had previously been neglected, but he points out that measurements by Bernett et al. [89], Buettner [90], and Wechsler and Glaser [91] indicate that this contribution is significant.

Dobar [41] concludes from his measurement of obsidian and pumice that K is also pressure dependent for solid rocks. Further, preliminary experiments by Wechsler [92] indicate that there is a gravity dependence which tends to reduce conductivity through an increase in contact resistance.

The failure of all models to accurately predict lunar thermal behavior and the possible dependence of thermal parameters on many variables suggest that a vastly more complex model is required. It is reasonable to assume that considerable inhomogeneity (both horizontal and vertical) exists, and that resolution limitations preclude an accurate evaluation through earth-based observations.

5.4. THERMAL ANOMALIES

Observation of the cooling of the lunar surface during an eclipse has indicated the existence of highly anomalous areas. During the eclipse of 12-13 March 1960, Shorthill et al. [93] verified the generally rapid cooling rate of the lunar surface, but discovered that the rayed craters Aristarchus, Copernicus, and Tycho were characterized by marked thermal anomalies. For example, a scan across Tycho during totality revealed temperatures as much as 60°K above the background of its environs. In all three cases, the anamoly was apparently confined to the crater area.

Sinton [94] observed Tycho in a 1.5-μ band at 8.8 μ during the total eclipse of 5 September 1960. Using a resolution of 27.9 (~52 km at the center of the disk), he observed "for the most part" with drift curves across the lunar disk, two of which are reproduced in figure 18a. The internal crater temperature was found to be 238°K and appeared to remain constant during totality. He makes no comment as to the geographical extent of the anomaly.

Sinton notes that of 17 craters examined at that time only Proclus failed to exhibit an anomalously high temperature. Observations by Saari and Shorthill [82] during the same eclipse,

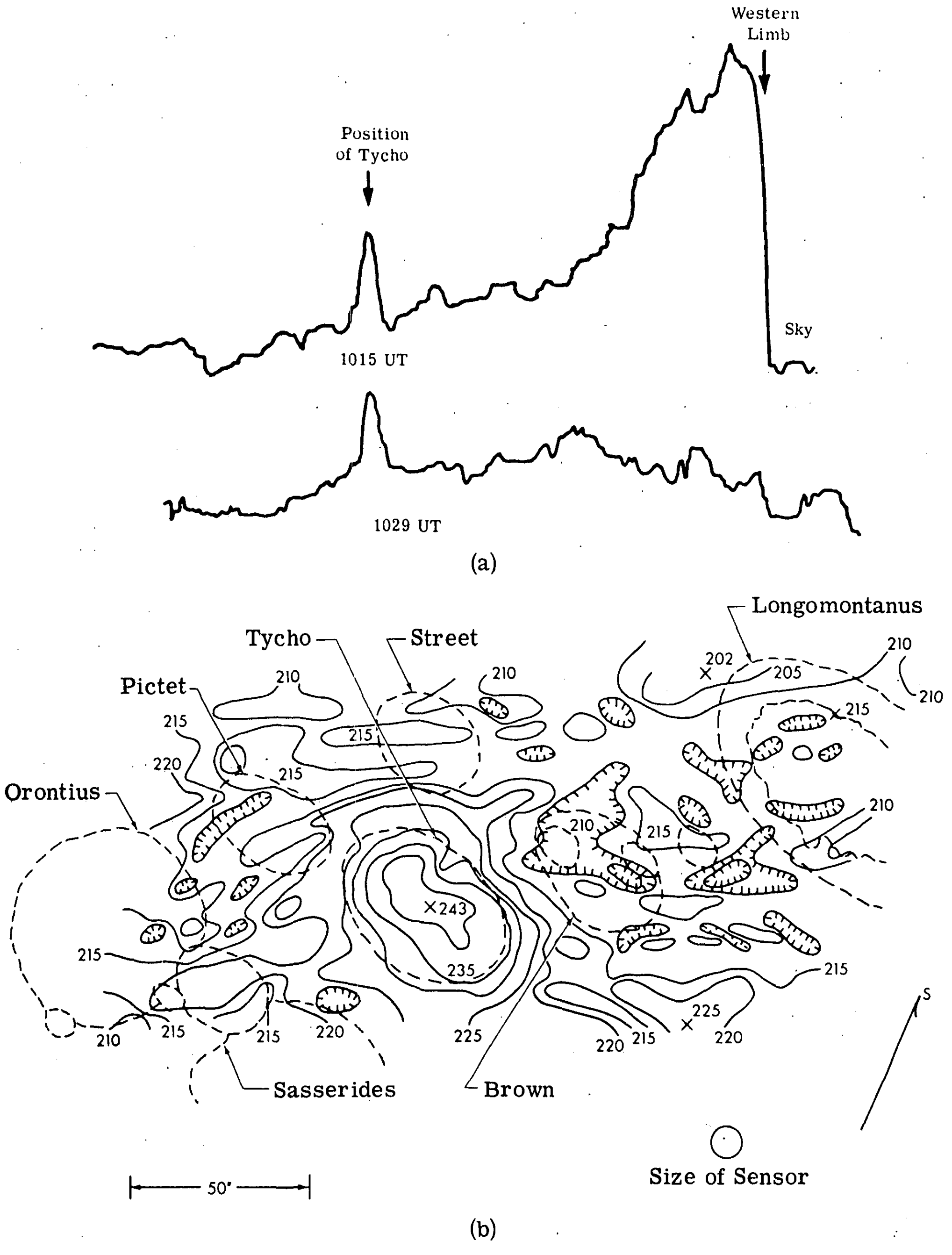

FIGURE 18. ISOTHERMS AND THERMAL SCANS OF TYCHO AREA. (a) Two scans across Tycho illustrating the rapid temperature decay of most of the moon's surface and the relative constancy of Tycho's temperatures during the eclipse [94]. (b) Isotherms in the region of Tycho during eclipse of 5 September 1960, 10:34 UT. Small circle indicates size of resolution element used; larger circle indicates size of that used by Sinton for scan in (a) [82].

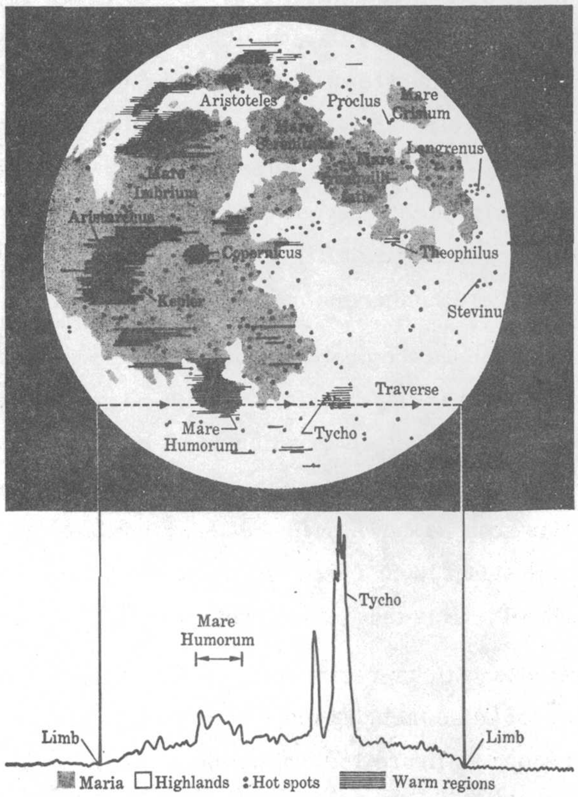

(c)

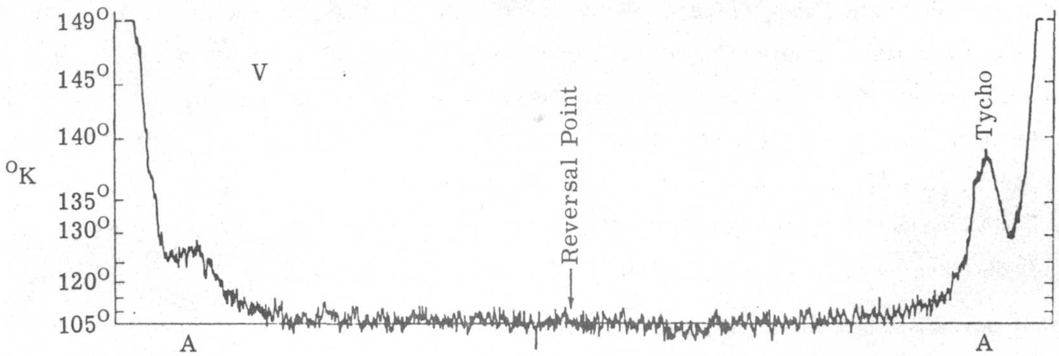

(d)

FIGURE 18. ISOTHERMS AND THERMAL SCANS OF TYCHO AREA. (Continued) (c) Map, produced by infrared scans of the eclipsed moon in December 1964, showing broad regions, concentrated in the maria, which stayed a few degrees warmer than their surroundings when the moon entered the earth's shadow, and local hot spots, mostly coincident with crators (as at Tycho), which stayed up to 48° hotter [96]. (d) Scan into the lunar nighttime across Tycho [55].

however, list Proclus as a definite thermal anomaly. They also observed Tycho essentially simultaneously with Sinton's observations (1034 UT and 1029 UT, respectively). The radiation detected in their observations was restricted to the infrared beyond 2 μ by a KRS-5 window and germanium filter. Their resolution was considerably better than that of Sinton, being 8 sec (~15 km). Saari and Shorthill quote a 31°K differential between the 243°K crater and the 212°K environs and indicate that the anomaly extends beyond the crater rim. Isotherms of the Tycho region are shown in figure 18b. Note in particular that the 238°K measured by Sinton at 8.8 μ is in almost exact agreement with these isotherms, considering his lower resolution.

Saari and Shorthill [95] again scanned the chord through Tycho during the total eclipse of 19 December 1964, this time utilizing a Ge:Hg detector at liquid-neon temperatures in the 10- to 12-μ band. The angular resolution for this observation was 10 sec (~19 km at the lunar surface). These data showed Tycho to be 226°K while the environs were only 178°K, a 48°K differential. The signal from this scan is shown in figure 18c, correlated with position along the chord. The three peaks in the signal from Tycho are possibly caused by the rims and central peak. The strong signal near Tycho is thought to emanate from the crater Heinsius A.

In addition to these eclipse observations, certain of the right ascension scans into the lunar nighttime by Murray and Wildey [55] also included the crater Tycho. An example of the signal received during such a scan is shown in figure 18d, where an anomaly in and around the crater is clearly indicated. Murray and Wildey state that it is definitely of larger geographic extent than the crater proper and exhibits considerable structure. Because of their near 50-km resolution, the apparent peak brightness temperature observed (138°K in the scan shown here) represents only a lower limit. Unlike the eclipse observations, which of necessity measure the cooling behavior after no more than 3 hr of total darkness, scans across the darkened disk during a normal lunation may involve periods of up to 14 days darkness near the limb. In this case, thermal properties of a much deeper layer of material can influence the measured surface temperature. A "thorough search" of the Tycho region by Murray and Wildey, 10 to 12 days into the lunar night, detected no anomalous temperature whatever.

The eclipse observation of Saari and Shorthill [82] in 1960 included only the five rayed craters, Aristarchus, Copernicus, Kepler, Proclus, and Tycho. However, during their 1964 observations, they were able to map the entire disk, localizing nearly 1000 thermal anomalies or "hot spots" [97]. These include not only the expected major rayed craters, but also other non-rayed craters, a rille (Hyginus Rille), bright areas such as near Linné, and extended areas in certain maria such as Mare Humorum (see fig. 18c and 19). They state that the anomalies are not distributed randomly over the surface (there is a concentration in Mare Tranquillitatis) [98].

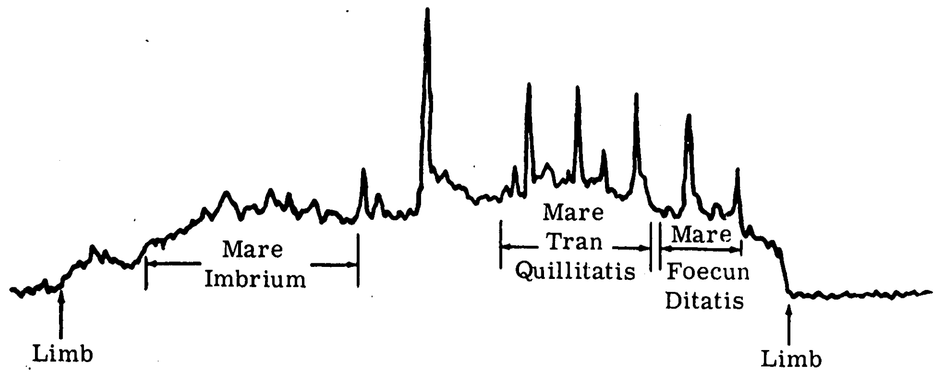

FIGURE 19. INFRARED SIGNAL DURING ECLIPSE COOLING SHOWING THERMAL ANOMALIES [95]

Listings of various anomalous areas tabulated by different observers can be found in the references given here. However, as an example of the extent and number of such areas, figure 20 shows 55 anomalies located in just the equatorial region of the visible disk between 5°N and 5°S latitude. Various reasons advanced to account for this anomalous cooling behavior include lower emissivity, enhanced thermal conductivity, a thinner insulating surface layer, a heterogeneous mixture of dust and bare rock, surface roughness, and subsurface heating.

Errors in lunar temperature measurements resulting from emissivity variations have been discussed by Burns and Lyon [100, 101, 102]. They state that errors in calculations based upon energy maxima as a function of wavelength can be as large as 65°K, while those for temperature differences in radiometric techniques can be on the order of 10°K. They conclude that the temperature changes reported by Shorthill and Saari could be caused entirely or in part by emissivity variations associated with compositional changes in surface material. Saari and Shorthill [82] consider this possibility but conclude it to be unlikely because of the large changes in emissivity required (on the order of 1.0 to 0.6 or less).

They also consider the favorite hypothesis of the volcanists, that of subsurface heating, and conclude that such an assumption requires a higher daytime temperature, whereas their observations indicate that anomalous cooling is in general associated with areas of cooler daytime temperatures. This evaluation of the case for subsurface heating as a cause of thermal anomalies has been referenced by Bastian [103] in his argument that hot spots result from surface roughness and by Murray and Wildey [55] in their deduction of an enhanced thermal conductivity. Unfortunately, while both of these conditions can reasonably be expected to contribute to anomalous thermal behavior, the argument of Saari and Shorthill does not seem to support them. On the contrary, in the absence of conductivity effects, the thermal inversion appears

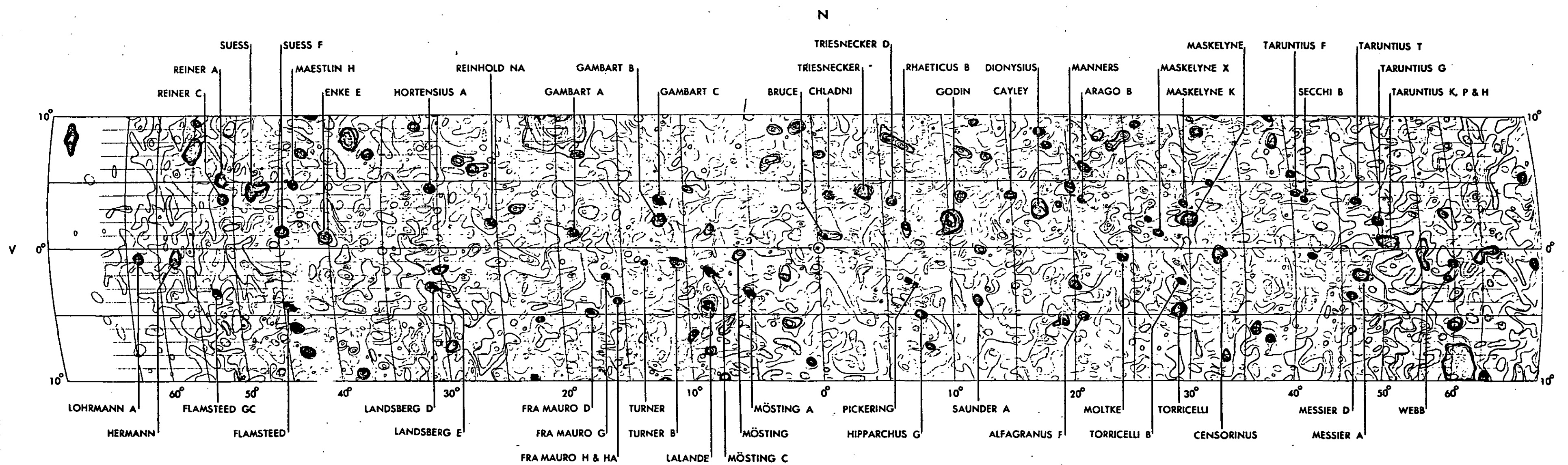

FIGURE 20. ISOTHERMAL CHART FOR LUNAR EQUATORIAL REGION DURING AN ECLIPSE. [99]
Contour intervals correspond to equal increments of signal in the 10- to 12-μ band. Craters between 5°N and 5°S latitude are identified.

to require (rather than preclude) either a rather large emissivity variation (considered unlikely by most observers) or subsurface heating. While the many unknowns such as spectral emissivity, surface and subsurface conductivity, and homogeneity preclude any definite conclusion in favor of subsurface heating, they also prevent its omission as a possibility.

The behavior of thermal anomalies as a function of time in darkness is a significant factor in the evaluation of possible causes. The limited duration of an eclipse, however, prevents an observation of cooling rates beyond an initial 3 to 4 hr. Such observations have detected a very rapid temperature drop during the penumbral phase, closely approximating that associated with an infinite thermal inertia. The temperature inversion between an anomalous feature and its environs occurs very early in this initial drop, and the consequent temperature differential appears to increase steadily until the beginning of totality. Both the anomalous feature and its environs exhibit an essentially constant temperature throughout totality (e.g., see the cooling curves for Aristarchus, fig. 16).

To investigate anomalous thermal behavior beyond this initial period requires observation of the darkened disk during a normal lunation. However, apparently because of the convenience of the higher temperatures involved, most observations of thermal anomalies have been made during an eclipse. As far as is known, no extensive studies of anomalous behavior at various phases of a lunation have been made.

Shorthill and Saari [56] reported a few scans across the darkened face of the 22-day-old moon, in which thermal anomalies were detected as far as 4 or 5 days into the lunar nighttime. Specifically, an anomalous differential of $20^{\circ}K$ to $25^{\circ}K$ was found to be associated with the crater De La Rue. No additional report concerning the behavior of this anomaly at other phases or of the detection of any anomalous behavior farther into the lunar nighttime is known at this time.

Murray and Wildey [55] report a thorough search of the Tycho area at a phase 10 to 12 days into the lunar night. During these final days of darkness, they were unable to detect any temperature differential associated with this feature, known to be highly anomalous during the early hours of cooling. Further, the data of figure 18d, obtained when Tycho was approximately 32 hr beyond the terminator, indicate a temperature differential of $20^{\circ}K$ (estimated from the figure). Eclipse data previously discussed show substantially larger differentials during totality.

Thus, pending a more thorough examination of the thermal behavior of known anomalous features as a function of time in darkness, preliminary data suggest a continued, although extremely slow, decrease in temperature to that of the environs. Such behavior, if verified, would constitute a strong argument against any appreciable subsurface-heating effect. This aspect of the anomalous cooling phenomenon seems significant and appears to have been largely ignored. Systematic investigations of thermal anomalies should be made throughout a lunation.

Assuming for the moment the disappearance of thermal anomalies with their advance beyond the terminator and the improbability of emissivity changes sufficient to account for the observed differences in temperature, we are left with surface roughness [103] and higher thermal conductivity as the most likely causes of anomalous cooling.

Murray and Wildey [55] infer the presence of more conductive materials, either in a heterogeneous surface mixture of dust and bare rock or overlain with a significantly thinner dust layer no more than a few millimeters thick. Sinton [94] came to a similar conclusion regarding his observations of Tycho. Through a comparison with the theoretical curves of Jaeger for both homogeneous and two-layer models, as well as a heterogeneous model of bare rock in dust, he deduced a layer of dust, 0.3 mm thick, on top of rock within the crater and a surface of thick dust for the environs. By assuming the thin dust layer to be the result of a cosmic infall at the same rate assumed by Whipple [104] for the earth, Sinton determined a maximum age of 10^7 years for Tycho.

Saari and Shorthill [82] point out that, because of a numerical error, this value should be reduced to 10^6 years. They have also considered a thin dust layer to account for their cooling data and calculate its thickness as only 0.075 mm within the crater. (The difference results primarily from a lower measured initial temperature.) Using this thickness and Whipple's estimate of cosmic infall, they arrive at an age of 0.27×10^6 years or only 1/4 that deduced by Sinton. Using an infall an order-of-magnitude higher, as estimated by Dubin and McCracken [105], they reduced the estimated age still further to only 0.027×10^6 years.

In summary, while anomalous thermal behavior is a well-established fact for many areas of the lunar disk, the interpretation of the data is subject to the same disagreement and lack of unanimity as is associated with other lunar measurements. Subsurface heating remains a possible, but unlikely, cause pending additional lunation measurements. Compositional emissivity changes alone do not appear sufficient to cause the large differentials observed. Variable thermal conductivity resulting from heterogeneous insulating properties appears to be the most plausible explanation at the present time.

6
RADAR OBSERVATIONS OF THE MOON

Through the visible and into the near-infrared portions of the spectrum, lunar radiation is predominantly the result of the reflection of solar illumination. At wavelengths longer than a few microns (depending upon lunar temperatures), self-emission begins to dominate. Because of the effect of the moon's temperature and terrestrial atmospheric absorption, this self-emitted radiation is present in detectable amounts to a wavelength on the order of a meter. The characteristics of the lunar surface as observed in these spectral ranges have been discussed in the preceding sections.

In order to study the behavior at longer wavelengths, it is necessary to illuminate the lunar surface artificially. However, it was only to satisfy the military needs of World War II that transmitter power and antenna capabilities were developed to the extent required to investigate the moon. In 1946, DeWitt and Stodola [106] (and days later, Bay [107]) first detected radar echoes from the moon using a wavelength of approximately 2.5 m.

Since these initial observations numerous experimental and theoretical studies of the characteristics of radar reflection from various surfaces have been performed. The result of these efforts has shown that, in general, radar returns are governed by certain equipment parameters such as wavelength and polarization and by the surface properties of roughness, electrical conductivity, and permittivity, as well as by the angle of incidence.

Radar return, in units of flux density received, may be described in terms of a surface reflection coefficient ρ and a directivity factor g, or in terms of an effective scattering cross section σ proportional to the product of these two.

A smooth, perfectly conducting sphere of radius significantly larger than the wavelength will reflect all incident energy ($\rho = 1$) isotropically ($g = 1$). Despite a growing "lunar hypothesis syndrome," we can be fairly certain the moon does not represent a perfect conductor and that the reflection coefficient will vary over the surface, being, on the average, substantially less than 1. Based upon the measured dielectric constant for dry terrestrial rocks and powders and the low lunar albedo, Evans [132] estimates ρ to be on the order of 0.1.

In the case of directivity (gain), isotropic reflection can occur only if the surface irregularities are smaller than about 1/8 wavelength. Such a degree of smoothness gives rise to specular reflection wherein only properly oriented (normal) surfaces can contribute to the observed return. In the terrestrial radar-moon situation, only the first few Fresnel zones at the front of the sphere would be effective in returning power to the receiver, producing a central bright area and distinct limb darkening. As will be discussed later, a similar situation is in fact observed.

In early considerations of lunar directivity, most analysts were prone to extrapolate from behavior observed at optical frequencies. Based upon optical measurements made during a lunation, Kerr and Shain [108] proposed a Lommel-Seeliger brightness distribution across the disk and deduced a value for g of 5.7, corresponding to irregularities having an average size much greater than the wavelength. They postulate that the absence of limb darkening in such a distribution resulted from advantageous reflection from mountain slopes near the limb. Grieg et al. [109] considered the distribution to be Lambertian (because of smaller surface irregularities, on the order of a wavelength in size) and obtained g ~ 2.7; such a model would exhibit some radar limb darkening. Winter [110], using the complex scattering law deduced by Pettit and Nicholson [49] from their infrared data, calculated a value for g of 2.5.

A reflection coefficient ρ for lunar materials can be calculated from measurements of the dielectric constant of similar terrestrial materials if a known composition is assumed. However, in the absence of an accurate knowledge of lunar composition and structure, radar returns yield only the product ρg from which an effective scattering cross section, $\sigma = \sigma(\rho g, \text{area})$, can be defined. This quantity then describes the ability of an illuminated area to reflect in a given direction.

A relatively poor resolution capability often causes radar returns to result from an average over the entire lunar disk or at best over several thousand square kilometers. As a result, the radar receiver cannot discriminate among the cross sections of individual scattering elements (σ_i) but rather averages the contribution of many elements into a "differential" scattering cross section per unit surface area (σ_0). It is the variation of this quantity with wavelength or polarization, normally expressed as a function of the angle of incidence, which provides a clue to lunar surface composition and structure.

Theoretical considerations of the variation in cross section have been reported by Spetner and Katz [111] in which they predict an inverse relation of the form $\sigma = k\lambda^{\alpha}$. A range of α from -6 to -2 was predicted for both isotropic scatterers and facet-like specular reflectors. Katz [112] has recently discussed this concept in terms of currently available data from terrestrial reflectivity experiments. He averaged the available data from what he termed "apparently similar surfaces" at a given angle of incidence and concluded that the variation of the exponent α with depression angle was characteristic of a particular surface. Resultant data illustrating the effects of wavelength, polarization, and angle of incidence on the radar return from common terrestrial materials are shown in figure 21. Note in particular the curve of figure 21c for the return from rough-sea clutter. While most surfaces exhibit the predicted negative exponent throughout the measurement range, in this case there is a crossover to positive values above a depression angle of 73° (17° from vertical). Katz states that at the larger (near-normal) depression angles, the return is due to specular reflection dependent upon the slope of wave facets, while at low depression angles (near grazing), it is due to diffuse scattering from smaller reflectors, resulting in a $\sin^n \theta$ law. Figure 21d illustrates experimental lunar radar data for two

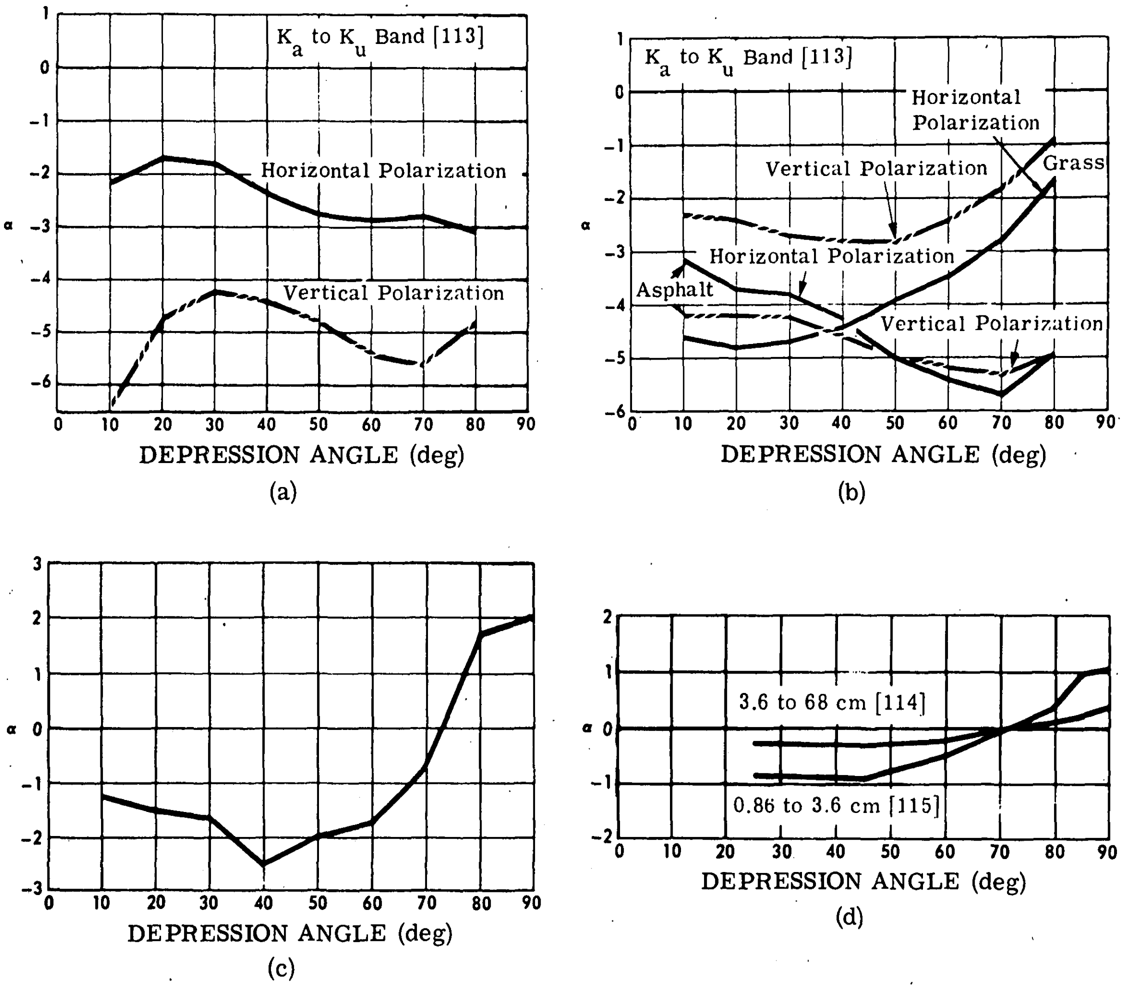

FIGURE 21. RADAR CROSS SECTION VS. WAVELENGTH FOR TERRESTRIAL AND LUNAR SURFACES. [112] (a) Wavelength dependence of concrete surface. (b) Comparison of wavelength dependence of asphalt and grass surfaces. (c) Wavelength dependence of sea clutter. This figure covers the microwave region from 0.86 to 71 cm and applies to rough-sea conditions. (d) Wavelength dependence of the moon's surface.

spectral bands. The significant feature is the crossover to positive α at 72.5°, similar to the sea-clutter case. The lower extreme values are attributed to an averaging process over large areas of the lunar surface; but the general shape and relation to sea clutter yield an insight into processes governing lunar radar reflection, and from this the nature of the surface structure.

For example, the experimental and theoretical data of figure 22 indicate that the scattering cross section of a smooth sea is high near vertical incidence but falls off rapidly with angle. The return from a geometrically similar surface (smooth desert) exhibits a smaller reflection

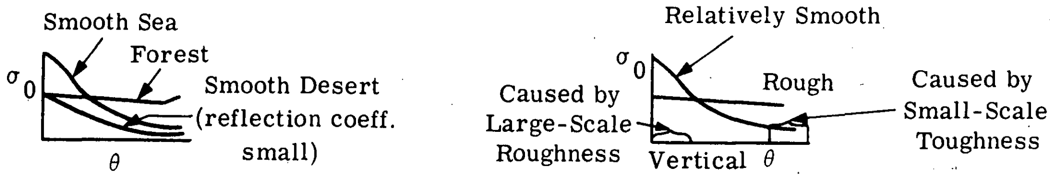

(a) Experimental Interpretation

(b) Theoretical Interpretation

FIGURE 22. RADAR CROSS SECTION VS. ANGLE OF INCIDENCE [116]

near vertical but a very similar behavior with angle of incidence. In contrast, the return from a surface of considerably rougher geometry (forest) exhibits the reduced vertical reflection but remains essentially constant with angle, producing a significantly larger return near grazing. Yaplee et al. [117] report that the specular-like reflection observed near the center of the lunar disk at 10 cm is similar to that which they observed from a dry, sandy desert at normal incidence.

In the discussion of surface roughness contributing to the lunar radar return, two basic models have been proposed. The first, based upon geometric optics, describes the surface in terms of plain flat facets (or possibly surface curvatures large in comparison with the wavelength [118]). Echoes are returned only from those facets which are properly oriented (perpendicular to the line of sight). Both the orientation and size of these facets are then described statistically by a probability law [111, 118-121]. In the alternative approach the lunar surface is normally described in terms of a Gaussian autocorrelation function of height vs. horizontal distance. This model represents the surface as gently undulating with height-deviating from the mean sphere according to a Gaussian distribution [121-128].

Both theoretical models appear to essentially ignore the effect of polarization and of penetration into the surface. However, these effects can be significant (cf. polarization effect in figs. 21a and 21b) and warrant inclusion. It is quite possible that the models attempt to represent subsurface phenomena in terms of surface features, resulting in, at best, difficult interpretation.

Another major problem in fitting lunar data to theoretical roughness models arises from librational motions of the moon, wherein the primary contribution to received echo power, that from the subterrestrial area, may result from relatively smooth or mountainous regions. If the moon remained fixed with respect to the observer, the received echo power, because of the combined effect of many scattering irregularities, would remain constant. However, a latitudinal libration (caused by the inclination between the lunar equator and its orbit), a longitudinal libration (caused by its elliptical orbit and rotational velocities), and a diurnal libration (caused by earth rotation) combine to alter the radar path lengths of various scatterers and consequently their phase-sensitive summation. As a result, the echo amplitude fluctuates (fades) with time. The initial echo detections of DeWitt and Stodola [106] and of Kerr and Shain [108] were seen to fade from pulse to pulse. The latter observers state that the rate was almost exactly that to be expected from the total libration if the moon behaved as a uniformly bright reflector.

The librational rotation will also result in a Doppler shift (f') in the return from strips parallel to the apparent rotation axis. The resulting distribution of echo power throughout the frequency range $\pm f_0'$ (i.e., the power spectrum) is related to the distribution of individual scatterers over the lunar disk. Further, the moon is a radar target of considerable depth (11.6 msec) and will therefore distort short pulses through interference between the returns from various scatterers. Hence the distribution of scattering centers over the lunar surface can be studied from the variation of echo intensity with time, $y(\tau)$, or with frequency, $y(f)$.

Browne et al. [129] and later Evans [130] studied the radio-frequency power spectrum in terms of a pulse-to-pulse autocorrelation function, $y(f_0', \tau)$. The fall in correlation of the amplitudes of successive pairs of pulses is compared to that anticipated from Lommel-Seeliger and Lambert scattering in figure 23a. Because of the obviously slower fading, Evans fitted a Gaussian exponential to his experimental data (also shown in fig. 23a). He further computed the associated power spectrum of such an autocorrelation function (compared to other scattering modes in fig. 23b) and concluded from the relatively small Doppler broadening that the major scattering

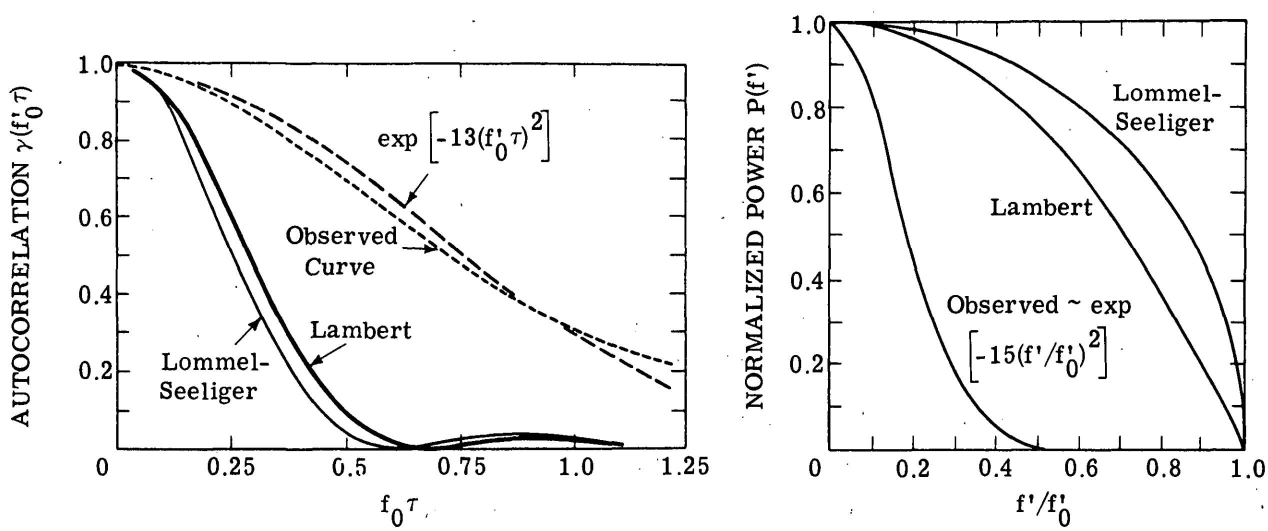

(a) Autocorrelation Function (b) Power Spectra

FIGURE 23. AUTOCORRELATION FUNCTION AND POWER SPECTRA FOR VARIOUS SCATTERING MODELS [130]

centers contributing to the return at 2.5 m wavelength lie within a central area with a radius about 1/3 that of the moon. This area, only 0.7 msec deep, is bordered by a pronounced dark limb, described by Evans (based upon the limb darkening of a Lambert, $\cos\phi$ law) as a $\cos^m \phi$ scattering. A similar relation ($\sin^n \theta$) was proposed by Katz to describe the scattering behavior of a rough sea surface. Evans deduced m = 30 for his power spectra.

In contrast to Evan's study of the distribution of scatterers through the frequency function y(f), Trexler [131] studied the time function $y(\tau)$ with short (12-μsec) pulses. He concluded that 50% of the echo power was returned within the first 50 μsec from a region only 210 mi in diameter, about 1/10 the radius of the moon (see fig. 24). Hey and Hughes [133] compared the echo intensity of 10-cm waves with inclination of the lunar surface to line of sight and concluded that 50% of the returned power came from regions inclined less than 5^o. This is said to be the result of a 2π-rad phase change through a lineal distance on the order of 1 m corresponding to a surface gradient of about 1 in 20.

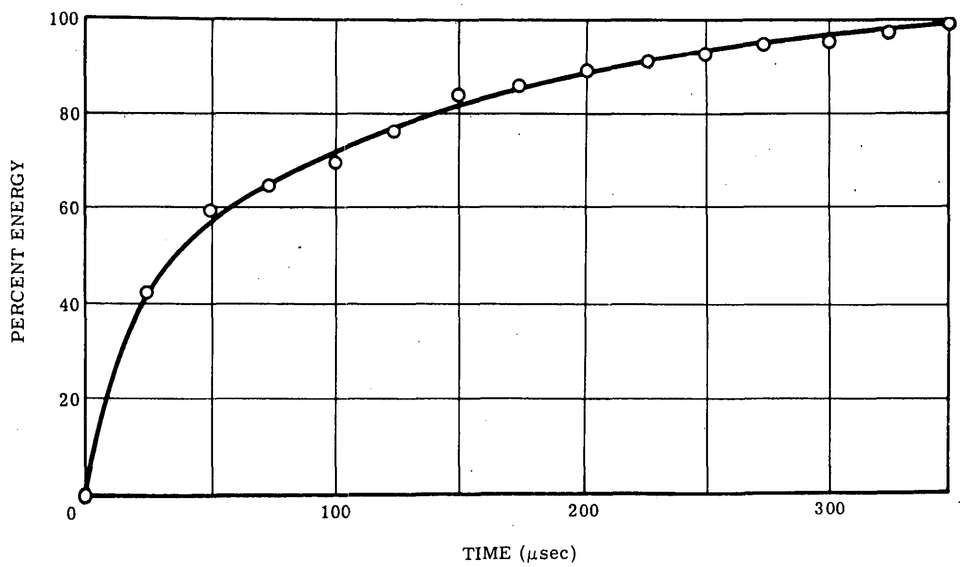

FIGURE 24. DISTRIBUTION OF ENERGY IN RADAR ECHO VS. TIME. Observed by Trexler [131] using 12-μsec transmitter pulses. More than 50% of the echo power is returned within the first 50 μsec. [132]

Evans [132] concluded from these experiments that lunar returns are principally from a specular reflection near the center of the disk and that the surface is not densely covered by objects from 10 cm to 2.5 m. However, both Leadebrand [134] and Pettengill [135] have been able to detect two types of scattering from the lunar surface. The first is the sharply decaying leading-edge echo discussed above and the second is a weaker component seen to decay linearly and to extend to the limb (see fig. 25). While the former is primarily specular, the latter

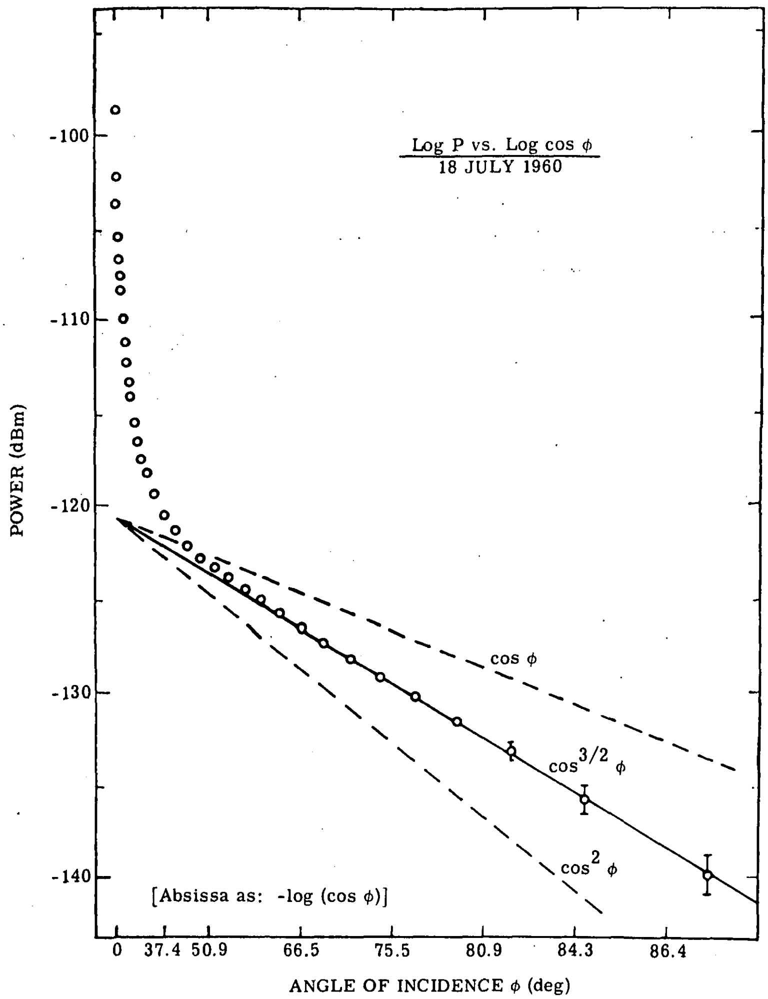

FIGURE 25. DISTRIBUTION OF ECHO POWER VS. ANGLE OF INCIDENCE FOR LUNAR SURFACE. Observed by Pettengill [135]; plotted as a function of the log of the cosine of the angle of incidence ϕ. For $\phi > 50^{o}$, the intensity of the echoes follows a law lying between the Lambert and the Lommel-Seeliger scattering laws. This law is similar to that observed by Pettit and Nichelson [49] at infrared wavelengths. [132]

appears to be nearly Lambertian, indicating that the surface is at least sparsely covered with irregularities on the order of a wavelength or more in size (70 cm in ref. 135). By comparing the relative magnitude of the two scattering components, Pettengill postulates that about 10% of the surface is rough at this wavelength.

Senior and Siegel [136] have tabulated the value of ρg given by various observers, from which Evans [132] concludes $\rho g = 7.6 \pm 2.1 \times 10^{-2}$. The value of g = 2.7 was calculated by Grieg et al. [109] for Lambertian scattering, which, according to Pettengill [135], constitutes about

10% of the return. Evans [132] postulates, therefore, a value $g = 1.3 \pm 0.1$ from which $\rho \sim 0.06$, corresponding to a dielectric constant of 2.72. The dielectric constant of dry, sandy soil (~2.5) is in close agreement, but that of silicate materials (~5) would require a bulk density of no more than 40% and indicate a porous, fragmented texture for the lunar surface [132, p. 470].

In summary, the scattering behavior of the lunar surface indicates a strong specular component wherein 50% of the echo power is returned from regions inclined less than 5° from perpendicular to the line of sight and confined to a central region of about 1/10 of the moon's radius. While most of the surface must be smooth and gently undulating with a gradient on the order of 1 in 20 [133] to 1 in 10 [132], it is probably sparsely populated with objects on the order of several centimeters to a few meters in size. Beyond a central region of about one-half of the moon's radius, these irregularities give rise to a detectable echo, functionally between Lambertian and Lommel-Seeliger.

This summary is apparently in excellent agreement with the photographs returned by Surveyor I of its landing site in Oceanus Procellarum, a site which bears a close resemblance to a barren, rock-strewn terrestrial landscape. Prior to direct, high-resolution observation by the Ranger and Surveyor probes, Evans [137] had concluded that the radar measurements of reflection coefficient indicate a surface covered by a thin layer of fine dust. However, Cudaback [138] used the same evidence to postulate a surface of cotton candy-like rock filaments rather than dust. These differences arise, in part, from the fact that radar measurements yield the product ρg rather than ρ directly. Only after inferring a value for directivity can we evaluate the reflection coefficient, which itself is dependent upon many variables such as composition, roughness, dielectric constant, and density. It is then necessary to infer certain facts about the first three to arrive at a low density, which may then be postulated as due to fine powders, filaments, vesiculation, etc.

Gold [5] notes that the remarkable smoothness deduced from measurements at wavelengths of at least a few centimeters compared to the roughness suggested at shorter wavelengths indicates a surface other than rock at a depth of "at least a few meters." His conclusion is based upon a presumed difficulty in generating and maintaining a rock surface of this smoothness in the presence of meteoritic bombardment.

However, the fact that certain rayed craters have been found to exhibit an enhanced radar return, as well as an anomalous cooling behavior, has been cited in favor of a rough, dense surface similar to bare rock. For example, by a combined range-Doppler drift analysis, Pettengill [8, 139, 140] has been able to observe an anomalously high radar return from the interior of the crater Tycho. This crater has already been discussed as an outstanding thermally anomalous area, which is further suggestive of bare rock or a very thin dust covering. However, as noted by Shorthill and Saari [98], several other rayed craters, such as Eratosthenes and Posidonius, exhibit an enhanced radar return but no detectable anomalous cooling behavior. Further, the fact that radar reflectivity contours show no simple correlation to eclipse-measured thermal data complicates the interpretation of both observations.

It must be concluded that, while radar measurements yield significant information concerning the nature of both surface and subsurface properties, there remains a considerable ambiguity in the interpretation of the details of both material and distribution. A major problem in this area is the lack of high-resolution coverage, which necessitates a sophisticated data analysis procedure to relate radar returns to specific surface features.

Moore et al. [141] have proposed a lunar orbiting radar package consisting of a 0.4-GHz scatterometer, an 8-GHz altimeter-scatterometer, and an 8-GHz imager which would eliminate the resolution limitation currently complicating the interpretation of earth-based data. They propose a resolution capability of 15 m for the imager and 1.6 to 15 km for the altimeter-scatterometer equipment. The imagery is expected to yield contours of dielectric constant and/or conductivity, using multiple polarization as well as map fracture systems, veneers, and possible subsurface structures. It is noted that radar imagery of terrestrial mountains has been able to detect and delineate fracture systems and folds which were not previously distinguished in aerial photographs or mapped in field surveys. The altimeter-scatterometer data are expected to give gross and fine structure features, measure slopes and roughness, and determine depth of penetration of multifrequency signals. The latter will aid in evaluating possible layering, subsurface features, permittivity, and conductivity. A multipolarization capability is also proposed to evaluate the possibility of depth-of-penetration analysis through non-uniform Brewster angle effects on vertically and horizontally polarized waves.

As noted in Moore's proposal, the major problem is not in the design of suitable radar equipment, but rather in the interpretation of the resulting data. We have currently only a general idea of the variation of radar return data with material composition, angle of incidence, polarization, and wavelength. Most airborne radar data have resulted from equipment development programs which did not involve close parametric control or extensive ground-truth data. The Ohio State data [113, and fig. 21a and 21b], while closely controlled, illustrate differences observed from laboratory-sized samples over areas of only a fraction of a square meter. An extensive study of radar return with respect to physical and chemical properties of the target material is needed, along with the development of display and interpretation techniques for multifrequency multipolarization data. The study presently underway at Kansas State University [141] will attempt to solve these problems and to deduce profiles and measure roughness characteristics, dielectric properties, layer thicknesses, etc., from radar measurements, as well as to develop means of display and interpretation of the data for geoscientific applications.

Appendix
REMOTE STUDY OF MINERALS BY SPECTRAL ANALYSIS IN THE INFRARED

Coblentz [142] in 1906 became one of the first workers to study minerals by infrared spectroscopy. Working in the 1- to 8-μ region, he determined that minerals exhibit characteristic absorption and reflection spectra. In 1938, Matossi and Bronder [143] studied the spectral reflectance of silicates, and later Pfund [144] utilized the diagnostic capabilities of 6- to 12-μ spectra in the identification of gems. A recent bibliography by McCarthy [145] lists many references to infrared spectral measurements. However, spectral reflectance studies have been primarily devoted to the study of glass and glass structures while emission measurements have largely involved heat transfer problems in high-temperature ceramics. Only a limited effort has been devoted to understanding the effect of composition, particle size, and structure upon the spectra of geological materials.

In 1953, Hunt and Turner [146] reported preliminary spectroscopic studies of the constituents of rocks. Frederickson and Ginsburg [147] and Bell et al. [148] have reported field measurements of spectral emission from terrain. The latter workers observed a distinct departure from blackbody behavior in the emission spectra of gypsum and silica sands (fig. 26). As noted by Burns and Lyon [101], the quartz reststrahlen of 9.08 μ is less pronounced than that seen in reflectance spectra. They suggest that this is the result of emission internal to the spectrometer, the ambient temperature of the sample (about 40°C) and an insufficient spectral resolution of about 25 cm^{-1} (0.25 μ), but add ". . . qualitative identification of sand-sized particles by remote infrared spectral measurements is possible . . . quartz and gypsum are clearly distinguishable from each other by the 0.49 micron wavelength shift of emission minimum" [101, p. 3772].

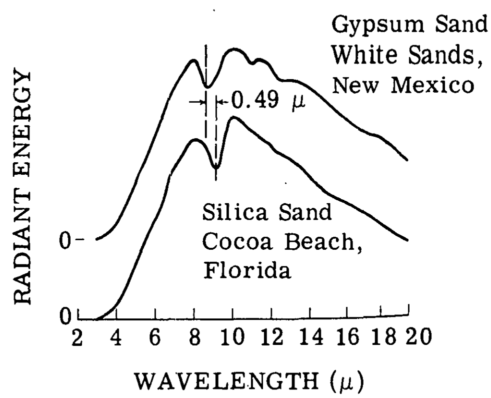

FIGURE 26. EMISSION CURVES FOR SANDS.
As observed by Bell et al. [148]. [101]

Using the results of these studies, Lyon [149] has proposed the use of infrared absorption, reflection, and emission spectra in the compositional analysis of geological assemblages. He has examined the absorption and reflection behavior of over 300 minerals and rocks in the 2- to 25-μ wavelength region. These materials range from acidic to ultrabasic, including various meteoritic specimens (fig. 27). Although the spectra of various samples are quite similar, certain characteristic differences are apparent, such as a shift in absorption maximum from around 1070 cm^{-1} for the acid rocks to 990 cm^{-1} for basic rocks (fig. 27a). A similar peak shift of about 160 cm^{-1} occurs between the reflectance spectra of tektite and a chondritic meteorite sample (fig. 27b). In both cases, these shifts were found to depend upon the bulk composition of the specimen but not its crystallinity, being exhibited by glassy, crystalline, fine-grained, and coarse-grained samples. Lyon concludes that the data demonstrate the feasibility of compositional analysis through reflection and absorption techniques.

In a remote analysis of the lunar surface, only emission spectra from materials in their natural (i.e., unprepared) state will be available. Lyon postulates that these emission spectra can be compared to those determined from a compilation of absorption and reflection data for various minerals. For a geological assemblage, the location of particular maxima and minima are expected to depend upon bulk composition, while the presence of specific minerals should be indicated by the more detailed fine structure of the spectral curve.

Because of experimental difficulties in a direct measurement of emission spectra, Burns [151] has discussed their derivation from reflectance measurements through the application of Kirchhoff's law to opaque, polished materials in thermal equilibrium. However, recent studies by Burns and Lyon [152] indicate that such a derivation may not apply to integrated measurements from a surface of very fine grained or powdery material. While the general shape of the spectral curve is maintained, deviations from graybody emission have been observed to decrease as particle size is reduced. Compositional differences are readily discernible for particle sizes on the order of 100 μ (in certain cases even <10 μ). However, as the particle size is further reduced, the surface approaches a graybody and spectral structure is obliterated.

Van Tassel and Simon [153] have pointed out that the application of this form of Kirchhoff's law is critically dependent upon material opacity (i.e., zero transmission). They propose the measurement of emission spectra of powders directly, rather than prediction from reflectance measurements, because of the inadequate knowledge of the nature and possible transparency of lunar surface materials. In measurements of two basic ranges of particle size (designated "flour" and "sand"), they also observed the dependence of identifying spectral characteristics upon particle size. Flour-sized samples (0.8 to 1.6 μ) of olivine and quartz exhibited very little unique band structure and closely approximated the emission of a graybody. Sand-sized particles

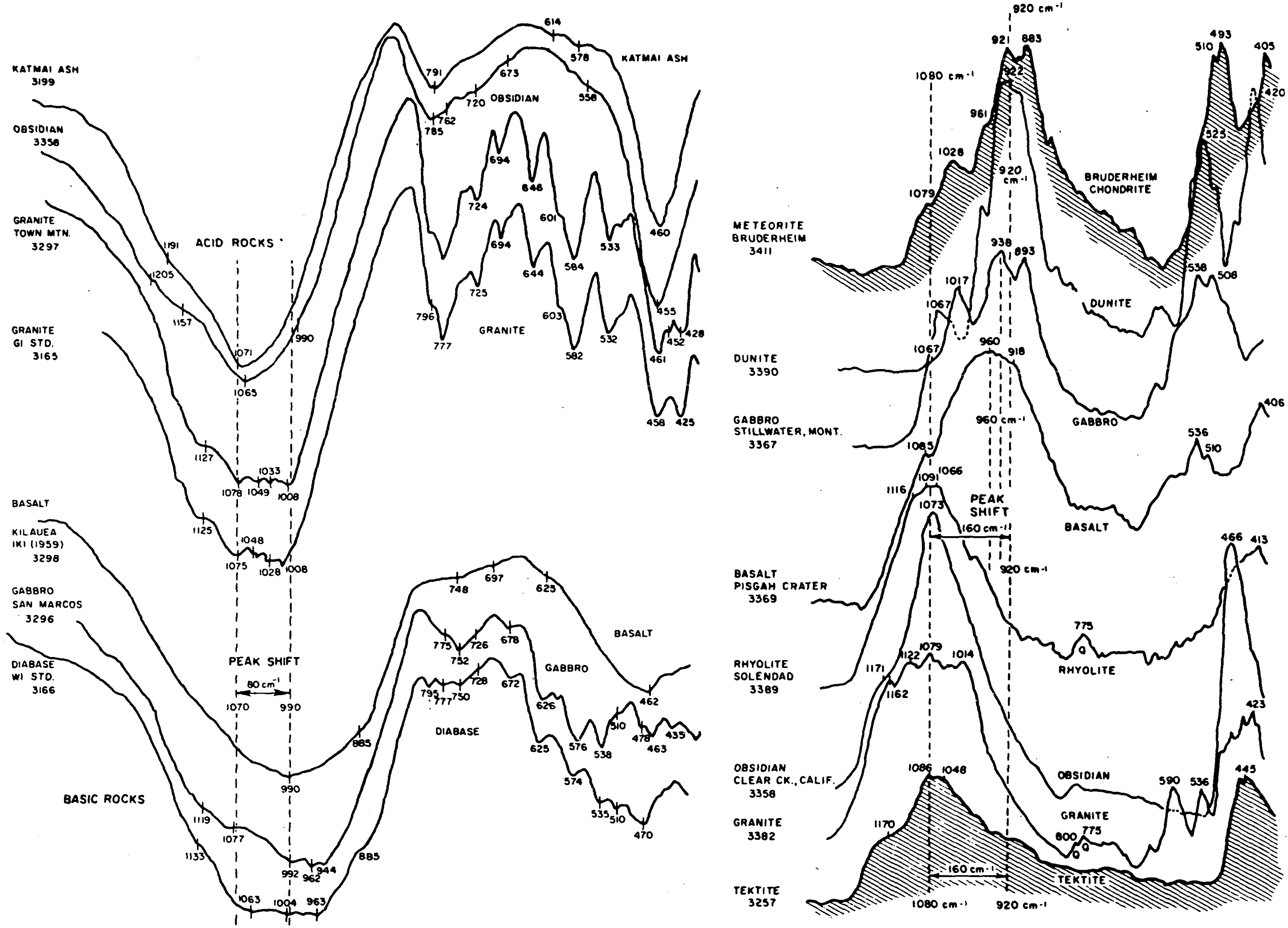

FIGURE 27. ABSORPTION AND REFLECTANCE SPECTRA OF VARIOUS MATERIALS. [150] (a) Comparison between absorption spectra for a group of acid rocks (upper four curves) and basic rocks (lower three curves). Sample sources are indicated. Ordinate is absorptance, with curves displaced vertically. Abscissa is in wavenumbers. Note the marked shift in peak position around 990 to 1070 cm^{-1}, between the two groups, regardless of the degree of crystallinity of the samples. (b) Peak shift of reflectance spectra of 160 cm^{-1} with rock compositions between tektite and chondritic meteorites. Ordinate is reflectance, with reference beam about 40% attenuated. Curves are displaced vertically. Abscissa is in wavenumbers.

(50 to 200 μ), however, produced distinctly recognizable spectral band patterns. Van Tassel and Simon conclude that if the actual size distribution of lunar surface particles corresponds to their "best estimate" (i.e., the flour samples) no diagnostic emission spectra can be obtained, but they add that the presence of a larger average particle size would make such compositional analysis feasible. They propose an examination of the spectral band structure in the emission from lunar surface materials as a potential means of determining particle size.

Hovis and Callahan [154] have reported spectral reflectance measurements of terrestrial materials in the 0.5- to 22-μ region. Their examination of various samples, in both solid and granulated form, confirmed the general observation that spectral contrast (beyond 8 μ) decreases as the particle size is reduced. However, they were able to detect considerable structure, particularly near wavelengths of 10 and 20 μ, for certain materials in particle sizes as low as 38 μ. They also observed a compositional shift of the fundamental Si-O vibration near 10 μ. The significant result of this study is their observation that at shorter wavelengths (below about 8 μ) the effect of particle size is reversed. Both the overall magnitude of reflectance and unique spectral detail are enhanced as particle size is reduced. Hovis [155, 156] has also demonstrated this effect in other studies and suggests that the pronounced change in reflectivity, particularly between 1 and 3 μ, may allow the determination of particle size. He further postulates that the observed enhancement of reflection features suggests the possibility of a more productive examination of lunar surface material by reflected than by emitted radiation.

As Hovis and Callahan [154] point out, the possibility of remote compositional analysis is certainly confirmed, but the situation is highly complex. The areal resolution of an orbiting spectrometer will likely include a variety of materials and particle sizes, and their total radiation will be integrated into a composite spectral curve. Various spectral shifts and diagnostic band structure may become confused or washed out entirely. At best, the data analysis and interpretation problems are immense.

While most spectral measurements have been made in the wavelength region below 25 μ, Aronson and McLinden [157] have extended this range to 200 μ for certain silicate materials. Because of the relative ease of reflectance measurements, they also invoke Kirchhoff's law for opaque materials to establish the applicability of reflectance spectra in this long-wavelength region. The effect of particle-size reduction upon diagnostic spectral detail was investigated with surfaces of fayalite powder filtered from a suspension of approximately 1-μ particles. By appropriate adjustment of spectroscopic variables to compensate for an overall reduction in reflectance and consequent signal-to-noise difficulties, they observe that "spectral detail remain" for this medium. It should be noted that their surface, while deposited from individually small particles, was not smooth to this degree. Irregularities are quite apparent, creating a surface macrostructure described as hillocks of an estimated height of 10 μ.

Spectral scans of certain lunar features in the 16- to 24-μ atmospheric window have been recorded by Hunt and Salisbury [158]. An area in the central highlands, Serenitatis, Copernicus, and Tycho were observed with an areal resolution of approximately 80 $\times$ 480 km and a spectral resolution of better than 0.4 μ. It is postulated that differences in mineral composition cause the discrepancies observed in the spectral emission from certain of the features. For example, at 19 μ the emission from Serenitatis is stronger than that from Copernicus, while at 23.5 μ the relative intensities are reversed (see fig. 28). Hunt and Salisbury state that the observed effect cannot result from differences in surface roughness, changes in atmospheric absorption, or temperature differences within a sampled area. Although the nature of the possible compositional anomaly is not understood, its detection adds significant weight to the argument for remote spectral analysis, particularly if the averaging effect of the large field of view (nearly 4×10^4 km^2) attainable in this earth-based observation is considered.

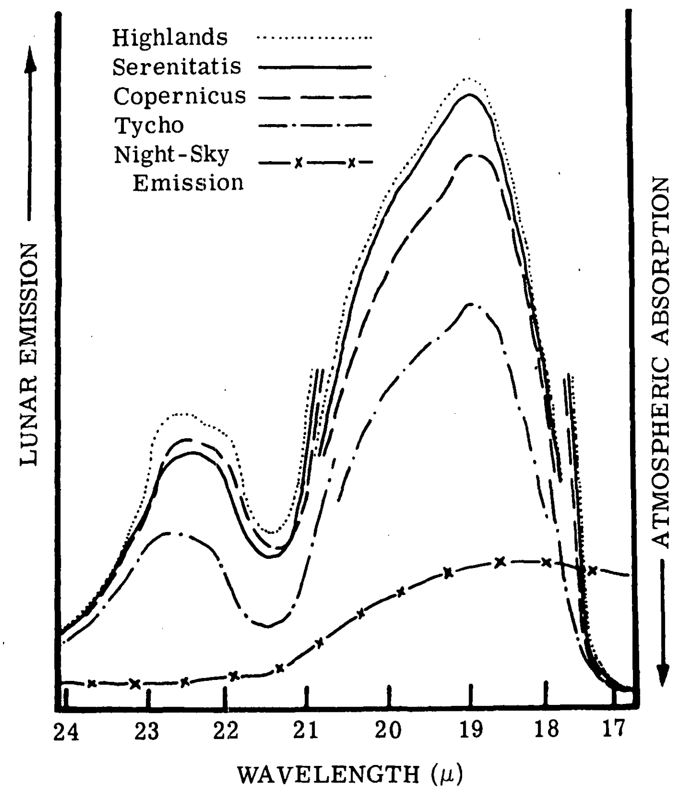

FIGURE 28. EMISSION SPECTRA OF LUNAR SURFACE FEATURES. Amplifier gain was 1.5 between 17 and 21 μ and 2.5 between 21 and 24 μ. [158]

Finally, the data returned by Surveyor I [7] suggest the feasibility of compositional analysis. The surface layer, at least near the landing site in Oceanus Procellarum, appears to be composed of a distinctly granular material as opposed to dust or powder. The wide size range includes a large number of blocks more than a meter across, scattered patches of rubble of smaller blocks, and finer grained material apparently of a basic grain size below the resolution limit of 0.5 mm. Significant concentrations of large blocks and finer rubble were detected, including areas strewn with very coarse, closely spaced blocks. It is concluded that "the mean grain size of surface material, averaged by particle mass, is probably on the order of about 1 mm" [7, p. 32]. While a basic grain size below 0.5 mm can be expected to predominate, the distinct granularity, apparent absence of dust or powdery material, and irregular distribution of large-block rubble should exhibit diagnostic spectral characteristics.

A more severe problem will probably arise from the simultaneous observation of various materials of different composition, particle size, and structure. The inherent confusion in spectral detail could preclude a meaningful geological analysis for certain lunar areas. However, for areas of a more uniform nature (at least a few resolution elements in extent), the potential of spectral techniques for a valid analysis appears to outweigh the inherent difficulties.

The phenomena and associated spectral regions of special interest include: the significant reflectance variation with particle size and complex compositional band structure between 1 and 3 μ; the shift of absorption maxima, Si-O vibrations, and general reststrahlen features near 10 μ; and the enhanced reflection and consequent departure from a graybody emission exhibited by many materials, even at reduced particle sizes, between about 19 and 25 μ.

REFERENCES

1. G. P. Kuiper, "The Moon," The Exploration of Space, ed. by R. Jastrow, Macmillan, 1960, pp. 70-76.
2. B. W. Hapke, "Photometric and Other Laboratory Studies Relating to the Lunar Surface," The Lunar Surface Layer, Materials and Characteristics, ed. by J. W. Salisbury and P. E. Glaser, Academic Press, 1964, pp. 323-354.
3. G. P. Kuiper, Interpretation of Ranger VII Records, Technical Report No. 32-700, Jet Propulsion Lab., California Institute of Technology, Pasadena, 1965 part II, chap. 3.
4. G. P. Kuiper, "Lunar Results from Rangers 7 to 9," Sky and Telescope, Vol. 29, May 1965, pp. 293-308.
5. T. Gold, The Implications of the Ranger Moon Pictures, Publication No. CRSR 176, Cornell University, Ithaca, N. Y., August 1964.
6. L. D. Jaffe, "Depth of the Lunar Dust," J. Geophys. Res., Vol. 70, No. 24, 1965, pp. 6129-6138.
7. Surveyor I, A Preliminary Report, NASA SP-126, National Aeronautics and Space Administration, Washington, June 1966.
8. V. G. Fessenkov, "Photometry of the Moon," Physics and Astronomy of the Moon, ed. by Z. Kopal, Academic Press, 1962, pp. 99-130.
9. Z. Kopal, Photographic Atlas of the Moon, Academic Press, 1965.
10. T. Gold, "Structure of the Moon's Surface," The Lunar Surface Layer, Materials and Characteristics, ed. by J. W. Salisbury and P. E. Glaser, Academic Press, 1964, pp. 345-354.
11. N. N. Sytinskaya, "Meteor-Slag Theory of the Lunar Surface," The Moon, ed. by Z. Kopal and Z. K. Mikhailov, Academic Press, 1962, pp. 391-394.
12. E. M. Shoemaker, "Interpretation of the Lunar Craters," Physics and Astronomy of the Moon, ed. by Z. Kopal, Academic Press, 1962, pp. 283-359.
13. B. W. Hapke and H. Van Horn, "Photometric Studies of Complex Surfaces, with Applications to the Moon," J. Geophys. Res., Vol. 68, No. 15, 1963, pp. 4545-4570.
14. G. K. Wehner, Sputtering Effects on the Moon's Surface, Report No. 2308, Electronics Group, General Mills, Inc., Minneapolis, 1962.
15. V. V. Sharanov, "Microrelief of the Lunar Surface and the Probable Ways of Its Formation," The Moon, ed. by Z. Kopal and Z. K. Mikhailov, Academic Press, 1962, pp. 385-390.
16. E. S. King, Harvard Ann., Vol. 85, No. 3, 1930, p. 45.
17. V. V. Sharanov, The Nature of the Planets, Moscow, 1958, p. 380.
18. V. V. Sharanov, "Some Results of Photometric and Colorimetric Comparison of Terrestrial Volcanic Crusts with the Lunar Surface," Geological Problems in Lunar Research, Ann. N. Y. Acad. Sci., Vol. 123, 1965, pp. 740-750.
19. N. N. Sytinskaya, "Photometric Data for and against the Presence of Widely Distributed Volcanic Activity on the Moon," Geological Problems in Lunar Research, Ann. N. Y. Acad. Sci., Vol. 123, 1965, pp. 756-767.

20. G. Galilei, "Dialogue about Two of the Great Systems of the World-Ptolmaic and Copernican," 1632, translated by S. Drake, University of California Press, Berkeley, 1953.

21. Bouguer, Traite d'Optique, 1729.

22. F. J. W. Herschel, Results of Astronomical Observations Made at the Cape of Good Hope, London, 1847.

23. W. C. Bond, Mem. Am. Acad. Arts Sci., NS. 8, 1861.

24. F. Zoellner, Photometrische Untersuchunger, Leipzig, 1865.

25. W. H. Pickering, Am. Harv. Coll. Obs., Vol. 61, 1908, p. 56.

26. H. N. Russell, Astrophys. J., Vol. 43, 1916, p. 103.

27. G. Rougier, "Photometrie Electronique Globale de la Lune," Ann. Obs. Strasbourg, Vol. 2, 1933, pp. 205-339.

28. T. Gehrels, T. Coffeen, and D. Owings, "Wavelength Dependence of Polarization, The Lunar Surface," Astron. J., Vol. 69, No. 10, 1964, pp. 826-852.

29. N. P. Barabashev, Astron. Nachr., Vol. 217, 1922, pp. 455-562.

30. A. Markov, Astron. Nachr., Vol. 221, 1924, pp. 65-78.

31. E. Öpik, "Photometric Measure on the Moon and the Earth Shine," Publ. Astron. Obs. Tartu, Vol. 26, 1924, pp. 1-68.

32. A. L. Bennett, "A Photovisual Investigation of the Brightness of 59 Areas on the Moon," Astrophys. J., Vol. 88, 1938, pp. 1-26.

33. J. van Diggelen, "Photometric Properties of Lunar Crater Floors," Rech. Obs. Utrecht, Vol. 14, 1959, pp. 1-114.

34. V. A. Fedoretz, "Photographic Photometry of the Lunar Surface," Publ. Kharkov Obs., Vol. 2, 1952, pp. 49-172.

35. R. L. Wildey and H. A. Pohn, "Detailed Photoelectric Photometry of the Moon," Astron. J., Vol. 69, 1964, pp. 619-634.

36. E. Schönberg, Acta Soc. Sci. Fennicae, Vol. 50, 1925, pp. 1-70.

37. V. A. Firsoff, The Strange World of the Moon, Basic Books, 1959.

38. L. G. Polgar and J. R. Howell, "The Directional Radioactive Characteristics of Conical Cavities and Their Relation to Lunar Phenomena," AIAA Paper No. 65-699, presented at the American Institute of Aeronautics and Astronautics Thermo-Physics Specialist Conference, Monterey, Calif., September 1965.

39. N. S. Orlova, Utch. Zap. Univ. Leningrad, No. 153, 1952.

40. B. W. Hapke, "A Theoretical Photometric Function for the Lunar Surface," J. Geophys. Res., Vol. 68, 1963, pp. 4571-4586.

41. W. I. Dobar, "Behavior of Lava on the Lunar Surface," Geological Problems in Lunar Research, Ann. N. Y. Acad. Sci., Vol. 123, 1965, pp. 495-515.

42. J. D. Halajian, "The Case for a Cohesive Lunar Surface Model," Geological Problems in Lunar Research, Ann. N. Y. Acad. Sci., Vol. 123, 1965, pp. 671-710.

43. P. Oetking, "Photometric Studies of Diffusely Reflecting Surfaces with Application to the Brightness of the Moon," J. Geophys. Res., Vol. 71, May 1966, pp. 2505-2513.

44. T. Gold, Monthly Notices Roy. Astron. Soc., Vol. 115, 1955, pp. 585-604.

45. B. W. Hapke, "Comments on Paper by Philip Oetking, 'Photometric Studies of Diffusely Reflecting Surfaces with Applications to the Brightness of the Moon'," J. Geophys. Res., Vol. 71, May 1966, p. 2515.

46. Lord Rosse, Proc. Roy. Soc., Vol. 17. 1869, p. 436.

47. S. P. Langley, Mem. Natl. Acad. Sci., Vol. 3, 1884, p. 3.

48. F. W. Very, Astrophys. J., Vol. 8, 1898, p. 265.

49. E. Pettit and S. B. Nicholson, Astrophys. J., Vol. 71, 1930, p. 102.

50. W. M. Sinton, "Temperatures on the Lunar Surface," Physics and Astronomy of the Moon, ed. by Z. Kopal, Academic Press, 1962, pp. 407-428.

51. W. M. Sinton and J. Strong, Astrophys. J., Vol. 131, 1960, p. 470.

52. J. M. Saari, "The Surface Temperature of the Antisolar Point of the Moon," Icarus, Vol. 3, 1964, pp. 161-163.

53. A. Adel, "Selected Topics in the Infrared Spectroscopy of the Solar System," Atmospheres of the Earth and Planets, ed. by G. Kuiper, University of Chicago Press, 1949.

54. H. J. Bolle, "The 15-26 Micron Sky Emission Spectrum at Jungfraujoch (3570 m)," Appl. Opt., Vol. 2, 1963, pp. 571-580.

55. B. C. Murray and R. L. Wildey, "Surface Temperature Variations during the Lunar Nighttime," Astrophys. J., Vol. 139, 1964, pp. 734-750.

56. R. W. Shorthill and J. M. Saari, "Radiometric and Photometric Mapping of the Moon Through a Lunation," Geological Problems in Lunar Research, Ann. N. Y. Acad. Sci., Vol. 123, 1965, pp. 722-739.

57. F. J. Low, "Lunar Observations at λ 10μ and 1.2 mm," Astron. J., Vol. 69, 1964, p. 143.

58. F. J. Low, "Lunar Nighttime Temperatures Measured at 20 Microns," Astrophys. J., Vol. 142, 1965, p. 806.

59. B. Gary, J. Stacey, and F. D. Drake, "Radiometric Mapping of the Moon at 3 Millimeters Wavelength," Astrophys. J. Suppl. Ser., Vol. 12, 1965, pp. 239-262.

60. R. H. Dicke and R. Beringer, Astrophys. J., Vol. 103, 1946, p. 275.

61. J. H. Piddington and H. C. Minnett, Australian J. Sci. Res. A., Vol. 2, 1949, p. 63.

62. F. J. Low and A. W. Davidson, "Lunar Observations at a Wavelength of 1 mm," Astrophys. J., Vol. 142, 1965, p. 1278.

63. J. L. Linsky, Models of the Lunar Surface Including Temperature Dependent Thermal Properties, Scientific Report No. 8, Harvard University Observatory, Cambrdige, Mass., 1966.

64. B. P. Jones, "Thermal Properties of the Moon as a Conductor of Heat," Physics of the Moon, ed. by G. C. Bucher and H. E. Stern, TN D-2944, National Aeronautics and Space Administration, Washington, 1965, pp. 121-124.

65. W. M. Sinton, J. Opt. Soc. Am., Vol. 45, 1955, p. 975.

66. J. J. Cook, L. G. Cross, and M. E. Bair, Willow Run Laboratories of the Institute of Science and Technology, The University of Michigan, Ann Arbor, unpublished single observation, 1961.

67. V. D. Krotikov and V. S. Troitskii, "Radio Emission and Nature of the Moon," Soviet Phys. Usp., Vol. 6, 1963, p. 841.

68. "Moon-Mars-Venus," Pravda, No. 345, 10 December 1961.

69. J. F. Denisse and E. LaRoux, in Seeger et al., Astrophys. J., Vol. 126, 1957, p. 585.

70. Z. Kopal, introduction to The Lunar Surface Layer, Materials and Characteristics, ed. by J. W. Salisbury and P. E. Glaser, Academic Press, 1964.

71. L. D. Russell, A Parametric Study of the Lunar Thermal Diffusivity Employing a Fourier Series, M-RP-INT-63-11, Marshall Space Flight Center, Huntsville, Ala., 1963.

72. J. E. Carson, Soil Temperature and Weather Conditions, Report No. ANL-6470, Argonne National Laboratory, Argonne, Ill., 1961.

73. J. E. Gibson, Proc. IRE, Vol. 46, 1958, p. 208.

74. P. Epstein, Phys. Rev., Vol. 33, 1929, p. 269.

75. A. J. Wesselink, Bull. Astron. Inst. Neth., Vol. 10, 1948, p. 356.

76. J. C. Jaeger, Proc. Camb. Phil. Soc., Vol. 49, 1953, p. 355.

77. J. C. Jaeger and A. F. A. Harper, "Nature of the Surface of the Moon," Nature, Vol. 166, 1950, p. 1026.

78. H. Lettau, "On the Heat Budget of the Moon and the Surface Temperatures during a Lunar Eclipse," Geofis. Pura Appl., Vol. 19, 1951, p. 1.

79. E. Pettit, Astrophys. J., Vol. 91, 1940, p. 408.

80. J. C. Jaeger, Australian J. Phys., Vol. 6, 1953, p. 10.

81. J. H. Fremlin, Nature, Vol. 183, 9 May 1959, p. 1317.

82. J. M. Saari and R. W. Shorthill, "Isotherms of Crater Regions on the Illuminated and Eclipsed Moon," Icarus, Vol. 2, 1963, pp. 115-136.

83. V. D. Krotikov and O. B. Shchuko, "The Heat Balance of the Lunar Surface Layer During a Lunation," Soviet Astron.—A. J., Vol. 4, No. 2, September-October 1963, pp. 228-232.

84. J. E. Gibson, "Lunar Surface Characteristics Indicated by the March 1960 Eclipse and Other Observations," Astrophys. J., Vol. 133, 1961, pp. 1072-1080.

85. A. G. Kislyakov, "Results of an Experimental Study of Lunar Radio Emission at 4 mm.," Soviet Astron.—A. J., Vol. 5, 1961, pp. 421-422.

86. C. F. Lucks et al., "The Experimental Measurement of Thermal Conductivities," Specific Heat and Densities of Metallic, Transparent, and Protective Materials, USAF Technical Report No. 6145, 1951.

87. R. W. Muncey, "Calculations of Lunar Temperature," Nature, Vol. 181, 1958, pp. 1458-1459.

88. W. C. Tyler and J. Copeland, "A Theoretical Model for the Lunar Surface," Astron. J., Vol. 67, 1962, p. 122.

89. E. C. Bernett et al., "Properties of a Simulated Lunar Material in Air and Vacuum," Am. Inst. Aeronaut. Astronaut. J., Vol. 1, 1963, p. 1402.

90. K. J. K. Buettner, "The Moon's First Decimeter," Planetary Space Sci., Vol. 11, 1963, p. 135.

91. A. E. Wechsler and P. E. Glaser, "Pressure Effects on Postulated Lunar Materials," Icarus, Vol. 4, 1965, p. 335.

92. A. E. Wechsler, Investigation of the Effects of Reduced Gravity on Thermal Properties of Insulation Materials, Report on Contract NAS 8-5413, Arthur D. Little, Inc., Cambridge, Mass.

93. R. W. Shorthill, H. C. Borough, and J. M. Conley, "Enhanced Lunar Thermal Radiation during a Lunar Eclipse," Publ. Astron. Soc. Pacific, Vol. 72, 1960, pp. 481-485.

94. W. M. Sinton, "Eclipse Temperatures of the Lunar Crater Tycho," The Moon, ed. by Z. Kopal and Z. K. Mikhailov, Academic Press, 1962, pp. 469-471.

95. J. M. Saari and R. W. Shorthill, "Thermal Anomalies on the Totally Eclipsed Moon of December 19, 1964," Nature, Vol. 205, 6 March 1965, pp. 964-965.

96. J. Green, "The Moon's Surface," International Science and Technology, September 1966, pp. 59-67.

97. J. M. Saari and R. W. Shorthill, "Hot Spots on the Moon," Sky and Telescope, Vol. XXXI, No. 6, June 1966.

98. R. W. Shorthill and J. M. Saari, "Non-Uniform Cooling of the Eclipsed Moon: A Listing of Thirty Prominent Anomalies," Science, Vol. 150, October 1965, pp. 210-212.

99. J. M. Saari and R. W. Shorthill, Isotherms in the Equatorial Region of the Totally Eclipsed Moon, Document No. D1-82-0530, Scientific Research Laboratory, Boeing Co., Seattle, April 1966.

100. R. J. P. Lyon and E. A. Burns, "Infrared Spectral Analysis of the Lunar Surface from an Orbiting Spacecraft," Proceedings of the Second Symposium on Remote Sensing of Environment (15, 16, 17 October 1962), Report No. 4864-3-X, Institute of Science and Technology, University of Michigan, February 1963, pp. 309-327.

101. E. A. Burns and R. J. P. Lyon, "Errors in the Measurement of the Lunar Temperature," J. Geophys. Res., Vol. 69, September 1964, pp. 3771-3778.

102. E. A. Burns and R. J. P. Lyon, "Errors in the Measurement of the Temperature of the Moon," Nature, Vol. 196, 1962, pp. 463-464.

103. J. A. Bastin, "Lunar Hot Spots," Nature, Vol. 207, September 1965, pp. 1381-1382.

104. F. L. Whipple in The Exploration of Space, ed. by R. Jastrow, Macmillan, 1960, p. 7.

105. M. Dubin and C. W. McCracken, "Measurements of Distribution of Interplanetary Dust," Astron. J., Vol. 67, 1962, pp. 248-256.

106. J. H. DeWitt and E. K. Stodola, Proc. IRE, Vol. 37, 1949, p. 229.

107. Z. Bay, Hung. Acta Phys., Vol. 1, 1946, p. 1.

108. F. J. Kerr and C. A. Shain, Nature, Vol. 179, 1957, p. 433.

109. D. D. Grieg, S. Metzger, and R. Waer, Proc. IRE, Vol. 36, 1948, p. 652.

110. D. F. Winter, TR-56-106, Air Force Cambridge Research Center, 1956.

111. L. M. Spetner and I. Katz, "Two Statistical Models for Radar Return," IEEE Trans. Antennas Propagation, Vol. AP-8, No. 3, 1960.

112. I. Katz, "Wavelength Dependence of the Radar Reflectivity of the Earth and Moon," J. Geophys. Res., Vol. 71, 1966, pp. 361-366.

113. R. L. Cosgriff, W. H. Peake, and R. C. Taylor, "Terrain Scattering Properties for Sensor System Design," Ohio State Univ. Eng. Exp. Sta. Bull., Vol. 29, No. 3, 1960.

114. J. V. Evans and G. H. Pettengill, "The Scattering Properties of the Lunar Surface at Radio Wavelengths," The Moon, Meteorites and Comets, ed. by Middlehurst and Kuiper, University of Chicago Press, 1963, pp. 129-164.

115. V. L. Lynn, M. D. Sohigian, and E. A. Crocker, "Radar Observations of the Moon at a Wavelength of 8.6 millimeters," J. Geophys. Res., Vol. 69, 1964.

116. R. K. Moore, "Radar Scatterometry—An Active Remote Sensing Tool," Proceedings of the Fourth Symposium on Remote Sensing of Environment (12, 13, 14 April 1966), Report No. 4864-11-X, Willow Run Laboratories of the Institute of Science and Technology, The University of Michigan, Ann Arbor, June 1966, pp. 339-373.

117. B. S. Yaplee et al., Proc. IRE, Vol. 46, 1958, p. 293.

118. D. G. Rea, N. Hetherington, and R. Mifflin, "The Analysis of Radar Echoes from the Moon," J. Geophys. Res., Vol. 69, 1964, pp. 5217-5223.

119. W. E. Brown, "A Lunar and Planetary Echo Theory," J. Geophys. Res., Vol. 65, 1960, pp. 3087-3095.

120. D. O. Muhleman, "Radar Scattering from Venus and the Moon," Astron. J., Vol. 69, 1964, pp. 34-41.

121. T. Hagfors, "Relationship of Geometric Optics and Auto Correlation Approaches to the Analysis of Lunar and Planetary Radar," J. Geophys. Res., Vol. 71, 1966, pp. 379-383.

122. H. Davies, "The Reflection of Electromagnetic Waves from a Rough Surface," J. Elec. Eng., Vol. 101, 1954, pp. 209-215.

123. J. K. Hargreaves, "Radio Observations of the Lunar Surface," Proc. Phys. Soc. (London), Vol. 73, 1959, pp. 536-537.

124. T. Hagfors, "Some Properties of Radio Waves Reflected from the Moon and Their Relation to the Lunar Surface," J. Geophys. Res., Vol. 66, 1961, pp. 777-785.

125. T. Hagfors, "Backscattering from an Undulating Surface with Applications to Radar Returns from the Moon," J. Geophys. Res., Vol. 69, 1964, pp. 3779-3784.

126. A. K. Fung, "Theory of Radar Scatter from Rough Surfaces, Bistatic and Monostatic with Applications to Lunar Radar Return," J. Geophys. Res., Vol. 69, 1964, pp. 1063-1073.

127. P. Beckman, "Radar Backscatter from the Surface of the Moon," J. Geophys. Res., Vol. 70, 1965, pp. 2345-2350.

128. A. K. Fung and R. K. Moore, "Effects of Structure on Moon and Earth Radar Returns at Various Angles," J. Geophys. Res., Vol. 69, 1964, pp. 1075-1081.

129. I. C. Browne et al., Proc. Phys. Soc. (London), Ser. B, Vol. 69, 1956, p. 901.

130. J. V. Evans, Proc. Phys. Soc. (London), Ser. B, Vol. 70, 1957, p. 1105.

131. J. H. Trexler, Proc. IRE, Vol. 46, 1958, p. 286.

132. J. V. Evans, "Radar Echo Studies of the Moon," Physics and Astronomy of the Moon, ed. by Z. Kopal, Academic Press, 1962, pp. 429-479.

133. J. S. Hey and V. A. Hughes, International Astronomy Union (Paris) Symposium on Radio Astronomy, Stanford University Press, 1959, p. 13.

134. R. L. Leadebrand et al., Proc. IRE, Vol. 48, 1960, p. 932.

135. G. Pettengill, Proc. IRE, Vol. 48, 1960, p. 933.

136. T. B. A. Senior and K. M. Siegel, J. Res. Natl. Bur. Std., Vol. 64D, 1960, p. 217.

137. J. V. Evans and G. H. Pettengill, "The Radar Cross-Section of the Moon," J. Geophys. Res., Vol. 68, 1963, pp. 5098-5099.

138. D. Cudaback, "Old Devil Moon," Newsweek, 15 April 1963, p. 62.

139. G. Pettengill and J. Henry, The Moon, ed. by Z. Kopal and Z. K. Mikhailov, Academic Press, 1962, p. 519.

140. P. E. Green and G. H. Pettengill, "Exploring the Solar System by Radar," Sky and Telescope, Vol. 20, 1960, pp. 9-14.

141. R. K. Moore et al., "The Use of an Imaging Radar and a Two-Frequency Altimeter-Scatterometer on Manned Orbiting Spacecraft to Investigate the Lunar and Terrestrial Surfaces," Proposal submitted to National Aeronautics and Space Administration, September 1965.

142. W. W. Coblentz, "Radiometric Investigations of Infrared Absorption and Reflection Spectra," Natl. Bur. Stds. (U. S.) Bull., Vol. 2, 1906, pp. 457-462.

143. F. Matossi and O. Bronder, "The Infrared Absorption Spectra of Several Silicates," Z. Physik, Vol. 111, 1938, pp. 1-17.

144. A. H. Pfund, "The Identification of Gems," J. Opt. Soc. Am., Vol. 35, 1945, pp. 611-614.

145. D. E. McCarthy, Appl. Opt., Vol. 4, 1965, pp. 507-509.

146. J. E. Hunt and J. S. Turner, "Determination of Mineral Constituents of Rocks by Infrared Spectroscopy," Anal. Chem., Vol. 25, 1953, pp. 1169-1174.

147. W. R. Frederickson and N. Ginsburg, Infrared Spectral Emissivity of Terrain, Internal Report No. 1 on Contract AF 33(616)-5034, Department of Physics, Syracuse University, 1957.

148. E. E. Bell et al., Infrared Techniques and Measurements, Final Engineering Report on Contract AF 33(616)-3312, Ohio State University Research Foundation, Columbus, 1957.

149. R. J. P. Lyon, Evaluation of Infrared Spectrophotometry for Compositional Analysis of Lunar and Planetary Soils, NASA TN-D-1871, April 1963.

150. R. J. P. Lyon and E. A. Burns, "Analysis of Rocks and Minerals by Reflected Infrared Radiation," Econ. Geol., Vol. 58, 1963, pp. 274-284.

151. E. A. Burns, "Background for Thermal Emissivity Studies," Appendix C in R. J. P. Lyon, Evaluation of Infrared Spectrophotometry for Compositional Analysis of Lunar and Planetary Soils, NASA-TN-D-1871, April 1963.

152. E. A. Burns and R. J. P. Lyon, "Feasibility of Remote Compositional Mapping of the Lunar Surface, Effects of Surface Roughness," The Lunar Surface Layer, Materials and Characteristics, ed. by J. Salisbury and P. Glaser, Academic Press, 1964, pp. 469-490.

153. R. A. Van Tassel, and I. Simon, "Thermal Emission Characteristics of Mineral Dusts," The Lunar Surface Layer, Materials and Characteristics, ed. by J. Salisbury and P. Glaser, Academic Press, 1964, pp. 445-468.

154. W. A. Hovis, Jr., and W. R. Callahan, "Infrared Reflectance Spectra of Igneous Rocks, Tuffs, and Red Sandstone from 0.5 - 22 Microns," Goddard Space Flight Center, Greenbelt, Md., unpublished paper, 1965.

155. W. A. Hovis, Jr., "Infrared Reflectivity of Iron Oxide Minerals," Icarus, Vol. 4, 1965, pp. 425-430.

156. W. A. Hovis, Jr., "Infrared Reflectance of Some Common Minerals," Appl. Opt., Vol. 5, February 1966, pp. 245-248.

157. J. R. Aronson and H. G. McLinden, "Far-Infrared Studies of Silicate Minerals," presented at the American Institute of Aeronautics and Astronautics Thermophysics Specialist Conference, Monterey, Calif., September 1965.

158. G. R. Hunt and J. W. Salisbury, "Lunar Surface Features: Mid-Infrared Spectral Observations," Science, Vol. 146, October 1964, pp. 641-642.

INDEX OF AUTHORS REFERENCED*

*The numbers refer to the preceding list of references and the number of the reference in the text.